Hydrol. Earth Syst. Sci. Discuss., https://doi.org/10.5194/hess-2017-707
Manuscript under review for journal Hydrol. Earth Syst. Sci.
Discussion started: 9 February 2018

Hydrology and Earth System Sciences
Open Access
Discussions

A comprehensive study of new hybrid models for Adaptive Neuro-Fuzzy Inference System (ANFIS) with Invasive Weed Optimization (IWO), Differential Evolution (DE), Firefly (FA), Particle Swarm Optimization (PSO) and Bees (BA) algorithms for spatial prediction of groundwater spring potential mapping

Khabat Khosravi[1], Mahdi Panahi*[2], Dieu Tien Bui*[3]

1-Department of watershed management engineering, Faculty of Natural Resources, Sari Agricultural Science and Natural Resources University, Sari, Iran.
2- Department of Geophysics, Young Researchers and Elites Club, North Tehran Branch, Islamic Azad University, Tehran, Iran. (E-mail: panahi2012@yahoo.com)
3- Geographic Information System Group, Department of Business and IT, University College of Southeast Norway,Gullbringvengen 36, 3800 Bø i Telemark, Norway. (E-mail: Dieu.T.Bui@usn.no)

Abstract

Groundwater are one of the most valuable natural resources in the world and their sustainable management is necessary. One of the most important methods in managing groundwater is developing groundwater potential mapping (GPM). The current study benefits from a new hybrids of Adaptive Neuro-Fuzzy Inference System (ANFIS) with five meta-heuristic algorithms, namely Invasive Weed Optimization (IWO), Differential Evolution (DE), Firefly (FA), Particle Swarm Optimization (PSO) and Bees (BA) algorithms for spatial prediction of groundwater spring potential mapping at Koohdasht-Nourabad plain, Lorestan province, Iran. A total number of 2463 springs were identified and then divided in two classes randomly, including 70% (1725 locations) of the springs were applied for model training and the remaining 30% (738 spring locations), which were excluded in the training phase, were utilized for the model valuation. Thirteen groundwater occurrence conditioning factors, namely slope degree, slope aspect, altitude, curvature, stream power index (SPI), topographic wetness index (TWI), terrain roughness index (TRI), distance from fault, distance from river, land-use, rainfall, soil order and lithology (units) have been selected for modeling. The stepwise assessment ratio analysis (SWARA) method was applied to determine the spatial correlation between springs and conditioning factors. The accuracy of the map achieved after applying these five hybrid models was determined using the area under the receiver operating characteristic (ROC) curve (AUC). The results showed that ANFIS-DE has the highest prediction capability (0.875) for groundwater spring potential mapping in the study area, followed by ANFIS-IWO and ANFIS-FA (0.873), ANFIS-PSO (0.865) and ANFIS-BA (0.839). Results of Freidman and Wilcoxon signed rank test revealed that there were statistically significant differences between the models' performances except for ANFIS-FA vs. ANFIS-DE and ANFIS-PSO vs. ANFIS-DE. The results of this research can be useful for decision makers to sustainable management of groundwater resources.

Key words: Groundwater spring, ANFIS-DE, ANFIS-IWO, ANFIS-FA, ANFIS-PSO, ANFIS-BA, Iran.

1. Introduction

Hydrol. Earth Syst. Sci. Discuss., https://doi.org/10.5194/hess-2017-707
Manuscript under review for journal Hydrol. Earth Syst. Sci.
Discussion started: 9 February 2018

Hydrology and Earth System Sciences
Discussions

Groundwater is defined as the water in a saturated zone which fills rock and pore spaces (Berhanu et al., 2014; Fitts, 2002) and groundwater potential is the possibility of groundwater occurrence in an area (Jha et al., 2010). The occurrence of groundwater in an aquifer is affected by various geo-environmental factors including lithology, topography, geology, fault and fracture and its connectivity, drainage pattern and land-use (Mukherjee, 1996). As one of the major conditioning factors, geological strata acts like a conduit and reservoir for groundwater. Storage and transmissivity of the formation has influence on the suitability of exploitation of groundwater in a given geological formation. Downhill and depression slopes impart runoff and improve recharge and infiltration, respectively (Waikar and Nilawar, 2014).

Groundwater which serves as a major source of drinking water to communities, for agricultural and for industrial purposes, is one of the most precious natural resources in the world (David Keith Todd and Mays, 1980) due to its consistent temperature, widespread availability, low vulnerability to pollution, low development cost and drought dependability (Jha et al., 2007). The life of about 1.5 billion people depends upon groundwater in the world solely for drinking purposes and about 38% of the irrigated lands depend on the groundwater itself (Siebert et al., 2013). As the population of mankind on earth increases, the demand for water constantly increases. The major challenge is sustainable management of groundwater to preserve and ensure continuous supply with regards to water demand. One of the most important measures for groundwater resource management is having adequate knowledge on spatial and temporal distribution of groundwater, its quantity as well as its quality. Approximately, two-third of Iran's area is covered by deserts. As a result, similar to other arid regions, the main sources of water supply for various uses, especially drinking, depends on the groundwater (Nosrati and Van Den Eeckhaut, 2012). Agriculture is one of the most prominent economic sectors in Iran and especially in the study area, limited by water scarcity (Zehtabian et al., 2010). Groundwater in Iran supplies around 65% of the water use-up and the remaining 35% is supplied by surface water (Rahmati et al., 2016). One of the most important measures to responsible for increase in fresh-water demand for drinking and agriculture is the identification of groundwater potential zoning as an essential tool for performing a successful groundwater determination, protection, and management program (Ozdemir, 2011a).

There are a number of methods for groundwater exploitation in traditional approaches including drilling as well as geological, geophysical, and hydrogeological methods. Yet, they are not only time-consuming and costly but uneconomical (David Keith Todd and Mays, 1980; Israil et al., 2006; Jha et al., 2010; Sander et al., 1996; Singh and Prakash, 2002). Recently, the application of geographic information systems (GIS) and remote sensing (RS) has become an effective procedure to groundwater potential mapping (Fashae et al., 2014) due to their ability in handling huge amount of spatial data, their easy performance and their applicability for being used in a lot of fields including water resources management, In more recent years, some probabilistic models such as frequency ratio (Oh et al., 2011), multi-criteria decision analysis (MCDA) (Kaliraj et al., 2014) (Rahmati et al., 2015) weights-of-evidence (WofE) (Pourtaghi and Pourghasemi, 2014), logistic regression (LR) (Ozdemir, 2011b; Pourtaghi and Pourghasemi, 2014), evidential belief function (EBF) (Nampak et al., 2014; Pourghasemi and Beheshtirad, 2015), decision tree (DT) (Chenini and Mammou, 2010), artificial neural network model (ANN) (Lee et al., 2012), and Shannon's entropy (Naghibi et al., 2015) have been used for recognition of groundwater potential mapping. The bivariate and multivariate statistical models have some disadvantages in measuring the relationship between groundwater occurrence and conditioning factors for the definition of statistical assumptions prior to the study (Tehrany et al., 2013; Umar et al., 2014). MCDA

technique is source of bias due to expert opinion. Traditional modeling approaches are also based on linear or additive modeling that is not consistent with natural process in the environment (Clapcott et al., 2013) but, machine learning models with non-linear structure handle data from various measurement scales and make no statistical assumptions; hence being useful for modeling applications such as GPM. ANN model is the most widely used model for environmental modeling among other machine learning models due to its computational efficiency (Bui et al., 2016; Ghalkhani et al., 2013; Rezaeianzadeh et al., 2014). The ANN model has a number of weaknesses such as poor prediction and error in modeling process (Bui et al., 2016). Thus, ANN model ensembles with fuzzy logic model and Adaptive Neuro-Fuzzy Inference System (ANFIS) model, which is a hybrid model proposed and used by some researchers due to its high accuracy (Güçlü and Şen, 2016; Lohani et al., 2012; Shu and Ouarda, 2008) (Chang and Tsai, 2016). It should be noted that even though ANFIS model has a higher accuracy than the two other model individually (Mukerji et al., 2009; Nayak et al., 2005), it has some disadvantages since it is weak in finding the best weight parameters affecting the prediction accuracy (Bui et al., 2016). These weights can be recognized using soft computing optimization process. Optimization problem is the problem of finding the best solution from among a set of all possible solutions.

The main aim of the current study is to carry out groundwater spring potential mapping (GSPM) in Koohdasht-Nourabad plain, Iran using ANFIS model, with some new metaheuristic models, namely Invasive Weed Optimization, Differential Evolution, Firefly, Particle Swarm Optimization and Bees algorithm which have some ensembles with ANFIS to solve the weakness of the ANFIS model. Another goal of the present study is drawing a comparison between prediction capabilities of these five new hybrid models in groundwater potential modeling in the study area as well. The main difference between the current study and the literature review is that these new hybrid models have not been used before for groundwater potential mapping, but their accuracy in prediction of landslide (Chen et al., 2017a) and flood (Termeh et al., 2018) susceptibility mapping has been confirmed recently. Since no such studies have been published so far in the study area, the current study is the pioneer work in this subject.

2. Case study description

Koohdasht-Nourabad Plain is located in the west part of Lorestan province, Iran. It lies between 33°3′ 28 and 34° 22′ 55 N latitudes and 46° 50′ 19 to 48° 21′ 18 E longitudes (Fig. 1). The region is located in the semi-arid area with mean annual precipitation of about 450 mm. The plain covers around 9531.9 km^2 with the population of 362,000 people (according to 2016 census). The occupation of most people living in the region is farming and water requirements are met through groundwater extraction. The altitude of the study area varies between 531 m and 3175 m above the sea level while the maximum and minimum slope is 0^o and 64^o, respectively. Geologically, the study area is located in Zagros structural zone of Iran and is mostly covered by Quaternary and Cretaceous-Paleocene geologic time scale. The dominant land-use of the study area is moderate forest (20%) and rocks covers the smallest area percentage (0.00067%). The residential areas also covers about 3% of the Koohdasht-Nourabad plain. Rock crop/Inceptisoils are the dominant soil types in the study area, covering about 51% of the study area.

Hydrol. Earth Syst. Sci. Discuss., https://doi.org/10.5194/hess-2017-707
Manuscript under review for journal Hydrol. Earth Syst. Sci.
Discussion started: 9 February 2018

Hydrology and Earth System Sciences
Discussions

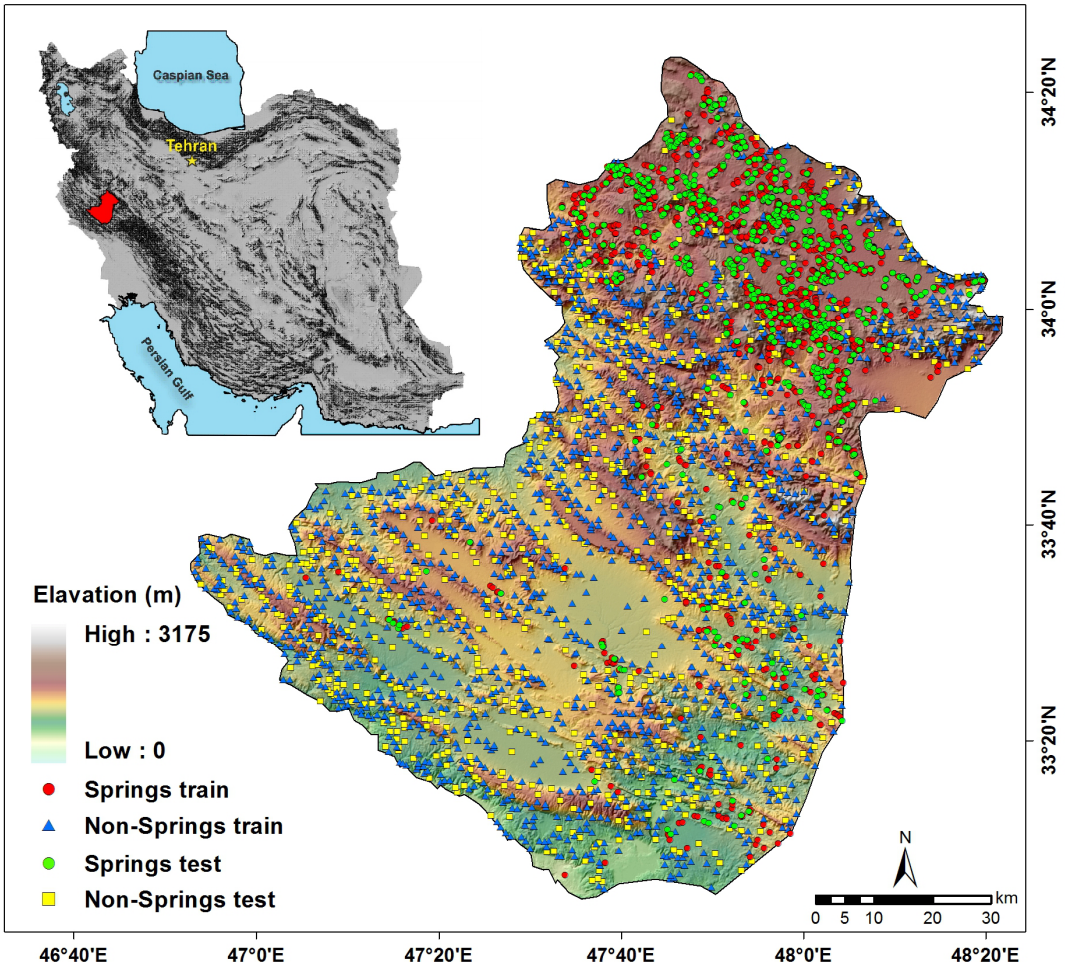

Fig.1. Groundwater well locations with DEM of the study area

3. Methodology

The methodological approach has been shown in Fig 2 and will be described step by step below.

Hydrol. Earth Syst. Sci. Discuss., https://doi.org/10.5194/hess-2017-707
Manuscript under review for journal Hydrol. Earth Syst. Sci.
Discussion started: 9 February 2018

Hydrology and Earth System Sciences
Discussions

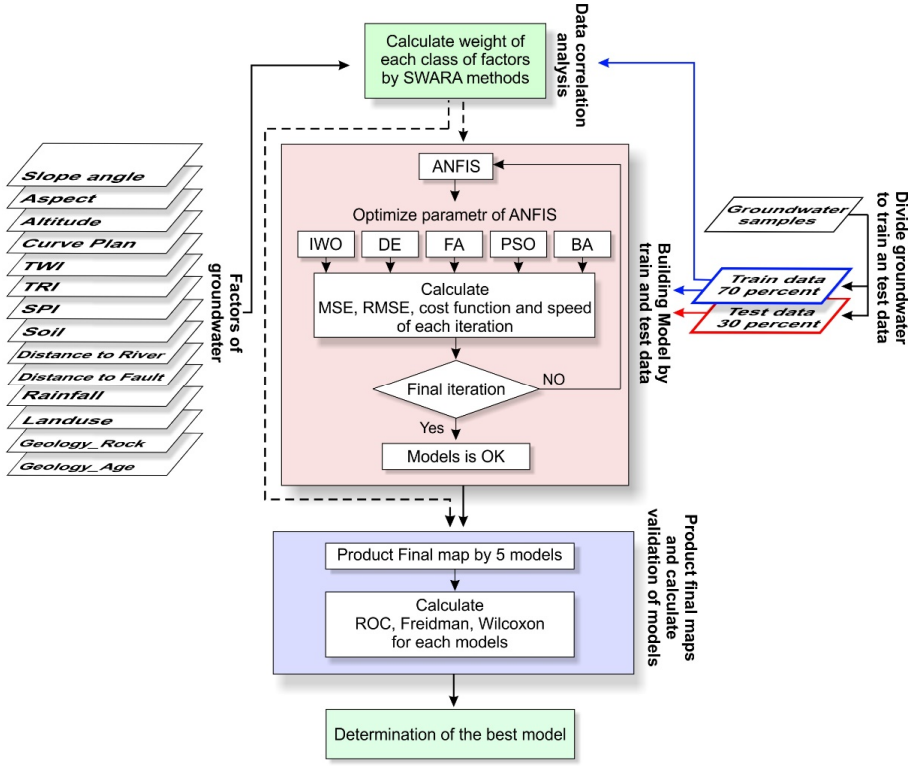

Fig.2. Conceptual model adopted in the current study

3.1. Data preparation

3.1.1. Groundwater spring inventory map

In any spatial prediction modeling such as groundwater modeling, spatial relationship between occurrence of groundwater springs and the conditioning factors should be analyzed. In Koohdasht-Nourabad plain, a total of 2463 springs were selected and considered for modeling. Most of the spring locations were checked using extensive field survey with GPS hand hole.

3.1.2. Construction of the training and validation dataset

Spatial prediction of groundwater potential mapping, using machine learning model, is a binary classification because the groundwater potential index is divided into two parts including spring location and non-spring location. Thus, 2463 non-spring locations were constructed randomly using created random point command in ArcGIS10.2. According to Chung and Fabbri (Chung and Fabbri, 2003), it is impossible to validate the model performance without considering the dataset for the two parts (Chung and Fabbri, 2003). The first part is used for model building which is also called training dataset and the other part is utilized for validating or testing the model performance which also called testing dataset (Pham et al., 2017a). In this study, a ratio of 70/30 was selected randomly for training and testing the dataset (Pourghasemi et al., 2013a; Pourghasemi et al., 2012; Pourghasemi et al., 2013b; Xu et al., 2012). Both spring location and non-spring location have

been divided into two groups for training (1725 location) and validating (738 location) purposes (Fig 1).

For building the training dataset, a total number of 1725 locations were randomly selected for both spring and non-spring location and were then combined with each other, and 738 of the remaining location of springs and non-springs were combined with each other again to construct the testing dataset. Finally, both training and testing datasets were converted to raster format and then overlaid with 13 groundwater conditioning factors. In both training and testing dataset, the spring pixels were assigned a value of 1 and non-spring pixels were assigned 0 (Bui et al., 2015).

3.1.3. Groundwater conditioning factor analysis

3.1.3.1. Selection of the Groundwater conditioning factor and multi-collinearity analysis

After definition of the effective factors, the conditioning factor should be assessed for multi-collinearity problem. Multi-collinearity takes place when two or more non-independence conditioning factors are highly correlated, or in other words inter-dependent (Li et al., 2010). Several methods have been proposed to multi-collinearity diagnoses from among which, two methods of Variance Inflation Factor (VIF) and tolerance are widely used for multi-collinearity problem recognition (Bui et al., 2016; O'brien, 2007). The VIF greater than 5 and tolerance less than 0.1 shows the multi-collinearity problem (Bui et al., 2011; O'brien, 2007).

In the current study, 14 conditioning factors have been selected including slope degree, slope aspect, altitude, curvature, stream power index (SPI), topographic wetness index (TWI), Terrain roughness index (TRI), distance from fault, distance from river, land-use, rainfall, soil order and lithology units. These factors have been selected according to the literature review, characteristics of the study area, and data availability (Mukherjee, 1996; Nampak et al., 2014; Oh et al., 2011; Ozdemir, 2011a), but there isn't any agreement on which the factors to be used for modeling. The process of converting continuous variables into categorical classes were carried out using expert opinions in order to define the class intervals (Bui et al., 2011). Digital Elevation Model (DEM) has been downloaded from ASTER global DEM with 30x30 m grid size and then slope degree, slope aspect, altitude, curvature, SPI, TWI and TRI have been constructed using DEM. Slope degree of the study areas varies between 0-64 degree. Slope factor has a direct impact on the runoff generation and therefore groundwater recharge, as the lower the slope, the lower runoff generation and the higher groundwater recharge. The slope degree has been divided in five categories using quantile classification scheme (Tehrany et al., 2013; Tehrany et al., 2014), including 0-5.5, 5.5-12.11, 12.11-19.4, 19.4-28.7, 28.7-64.3 degree (Fig 3a). Slope aspect is another factor that has affects the groundwater potential through solar radiation since the north aspect receives a lower sun light and as a result is less wet or has low evapotranspiration. The slope aspect has been provided in 5 different classes including, flat, north, west, south and east (Fig 3b). The third conditioning factor is altitude. It has been divided into five classes using quantile classification scheme including 531-1070, 1070-1385, 1385-1703, 1703-2068 and 2068-3175 m (Fig.3c). Curvature factor has been constructed using DEM and finally divided into three classes, namely concave (<−0.05), flat (−0.05–0.05), and convex (>0.05) (Fig.3d) (Pham et al.2017). SPI is the measurement of erosive power of surface runoff and TWI shows an amount of the flow that accumulates at any point in the catchment. TRI, topographic roughness or terrain ruggedness calculates the sum of change in elevation between a grid cell and its neighborhood. SPI, TWI and TRI have been constructed in the system for Automated Geoscientific Analyses (SAGA-GIS 2.2)

Hydrol. Earth Syst. Sci. Discuss., https://doi.org/10.5194/hess-2017-707
Manuscript under review for journal Hydrol. Earth Syst. Sci.
Discussion started: 9 February 2018

software and finally divided into five classes that are 0-48664, 48664-227099, 227099-583969, 583969-1330153, 1330153-4136452 (Fig.3e) for SPI, 2.1-4.6, 4.6-5.6, 5.6-6.6, 6.6-7.9, 7.9-11.9 (Fig.3f) for TWI, and finally 0-8.7, 8.7-18.2, 18.2-29.9, 29.9-46.6, 46.6-185 (Fig.3g) for TRI.

Distance from fault and river factors have been provided using fault and river of the study area via multiple ring-buffer command in ArcGIS10.2 software which is finally divided into five classes including: 0-200, 200-500, 500-1000, 1000-2000 and >2000 m (Fig. 3h and Fig. 3i). Lithology plays a key role in determining the groundwater potential occurrences due to different infiltration rate of formation that has been considered in some previous studies (Adiat et al., 2012; Nampak et al., 2014; Pradhan, 2009). Land-use of the study area has been provided through Landsat 7 Enhanced Thematic Mapper plus (ETM+) images downloaded from the US Geological Survey (USGS) and supervised image classification techniques (Lillesand et al., 2014). Finally, the accuracy of the land-use map has been controlled by filed surveys.

Twenty five land-use types including agriculture, garden, dense-forest, good rangeland, poor forest, waterway, mixture of garden and agriculture, mixture of agriculture with dry farming, mixture of agriculture with poor-garden, dry farming, follow, dense rangeland, very poor forest, mixture of waterway and vegetation, mixture of moderate forest and agriculture, mixture of moderate rangeland and agriculture, mixture of poor rangeland and follow, mixture of low forest and follow, wood-land, moderate forest, moderate rangeland, poor rangeland, bare soil and rock, urban and residential, mixture of very poor forest, and rangeland have been identified (Fig.3j). As the major source of recharge to the groundwater, rainfall has been provided via mean annual historical rainfall data of past 15 years (2000–2015) using 4 rain-gauge stations in the study area. Inverse distance weighted (IDW) method has been used for the preparation of the rainfall map due to lower RMSE than other methods and then, rainfall map of the study area has been divided into five categories including: 300-400, 400-500, 500-600, 600-700, 700-800 mm (Fig 3k). The soil properties directly affect the water infiltration rate as well as groundwater recharge. The 1:50000 soil map of Lorestan province obtained from the Iranian Water Resources Department (IWRD) has been used for the analysis. The soil map was in a polygon format which needed to be converted to grid. The most dominant feature of the study area is rock outcrop/Entisols, rock outcrop/Inceptisols, Inceptisols, Inceptisols/Vertisols and Badlands (Fig.3l).

Hydrol. Earth Syst. Sci. Discuss., https://doi.org/10.5194/hess-2017-707
Manuscript under review for journal Hydrol. Earth Syst. Sci.
Discussion started: 9 February 2018

Hydrology and Earth System Sciences
Discussions

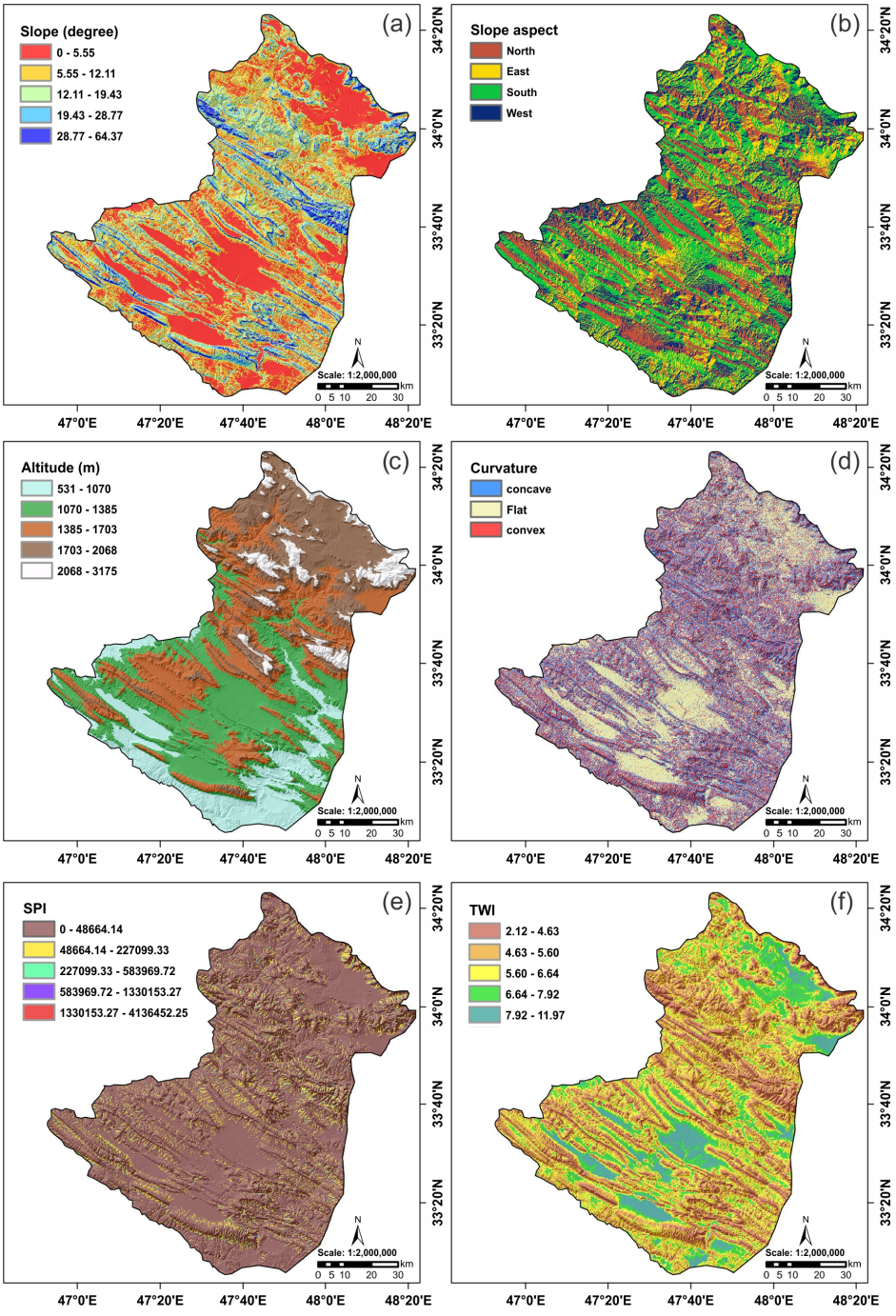

227

228 Fig.3. Thematic Groundwater conditioning factor in the study area: slope degree(a), slope aspect (b),
229 altitude (c), curvature (d), SPI (e), TWI (f), TRI (g), distance from fault (h), distance from river (i), land-
230 use (j), rainfall (k), soil order (l), and lithology units (m).

Hydrol. Earth Syst. Sci. Discuss., https://doi.org/10.5194/hess-2017-707
Manuscript under review for journal Hydrol. Earth Syst. Sci.
Discussion started: 9 February 2018

Hydrology and Earth System Sciences
Discussions

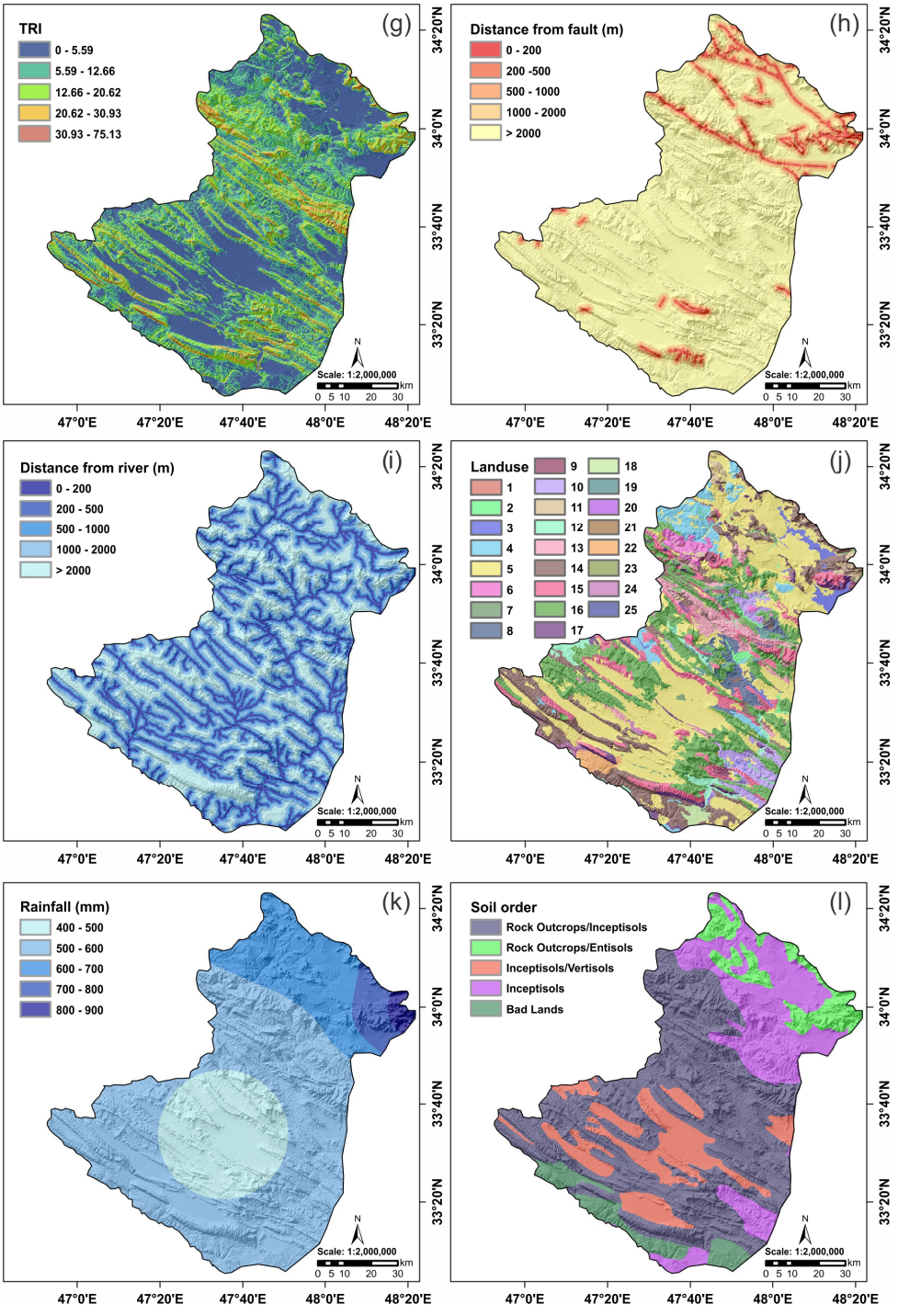

231

232 Fig.3.Continued

Hydrol. Earth Syst. Sci. Discuss., https://doi.org/10.5194/hess-2017-707
Manuscript under review for journal Hydrol. Earth Syst. Sci.
Discussion started: 9 February 2018

Hydrology and Earth System Sciences
Discussions

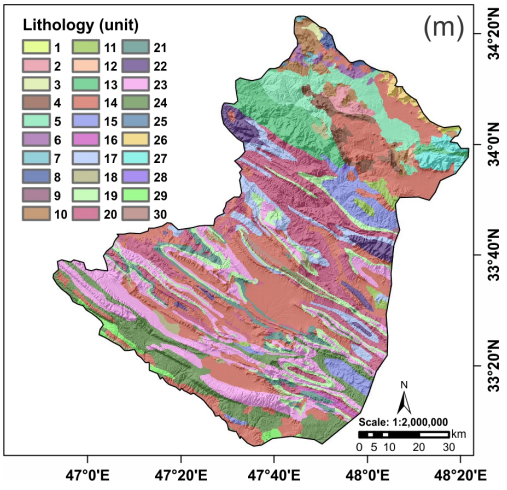

Fig.3. Continued

Finally, all the aforementioned groundwater conditioning factors for modeling purposes were converted to a raster grid with 30 m × 30 m pixel size in the ArcGIS 10.2 software. Lithology (unit) has a high influence on infiltration; thus, it has been considered in the current study. Lithology for the study area has been constructed in scale of 1:100000, which was created by Iranian Department of Geology Survey (IDGS) and divided into thirty classes including: OMq, PeEf, PlQc, K1bl, Plc, pd, TRKubl, TRJvm, MPlfgp, OMql, Plbk, E2c, TRKurl, Qft2, MuPlaj, KEpd-gu, Kgu, Qft1, Ekn, KPeam, PeEtz, Kbgp, EMas-sb, Mgs, TRJlr, Klsol, JKbl, Kur, OMas and Mmn (Fig.3m).

3.2. Spatial relationship between spring location and conditioning factors

Step-wise Assessment Ratio Analysis (SWARA) as a Multi-Criteria Decision Making (MCDM) was first introduced by Keršuliene in 2010 for the first time (Keršuliene et al., 2010) as a Multi-Criteria Decision Making (MCDM). Since this method is both simple and rooted on experts' views, it has drawn a lot of attention in diverse fields (Alimardani et al., 2013; Hong et al., 2017).

The specialist allocates respectively the highest and lowest rank from the most and least valuable criterion, respectively. Afterwards, the all-inclusive ranks are specified by the average value of ranks. SWARA's detail is illustrated in Fig 4.

Hydrol. Earth Syst. Sci. Discuss., https://doi.org/10.5194/hess-2017-707
Manuscript under review for journal Hydrol. Earth Syst. Sci.
Discussion started: 9 February 2018

Hydrology and Earth System Sciences
Discussions

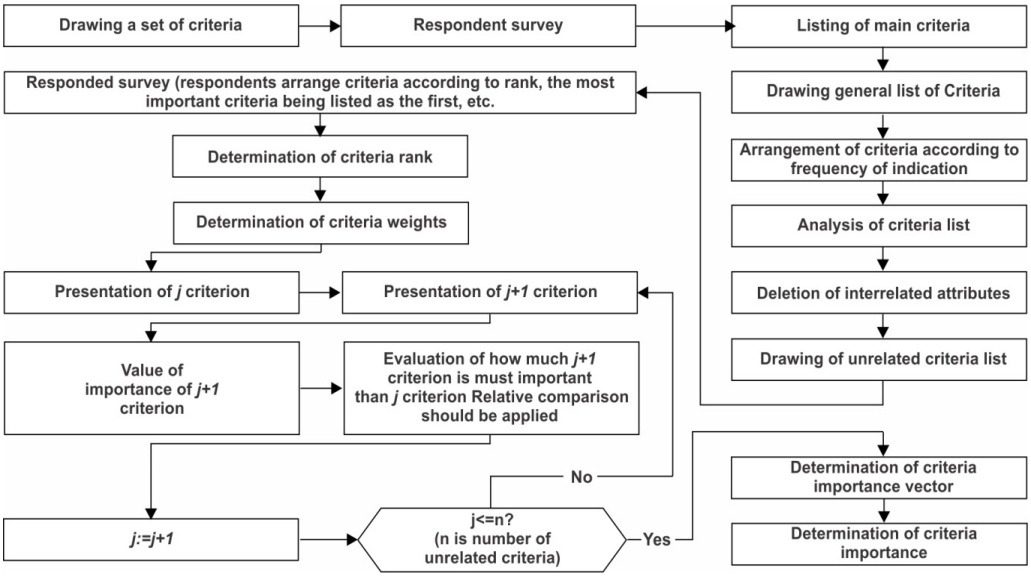

Fig4. the flowchart of SWARA method (Keršuliene et al., 2010)

The phases of method are as the following:

Phase one: for evolving decision making models, first, the experts define the problem solving criteria. By using the practical knowledge of the experts, the priority for each criteria are determined as well and the criteria are organized in descending order finally.

Phase two: regarding to each parameter's ranking, the following trend is employed for calculation of the weight in each criteria:

Starting from the second criterion, the respondent explains the relative importance of the criterion j in relation to the $(j-1)$ criterion, and for each particular criterion as well. As Keršuliene mentioned in his article, this process specifies the Comparative Importance of the Average Value, S_j as follows (Keršuliene et al., 2010):

$$S_j = \frac{\sum_i^n A_i}{n} \tag{1}$$

Where n is the number of experts; A_i explicates the offered ranks for each factor by the experts; j stands for the number of the factor.

Subsequently, the coefficient K_j is determined as follows:

$$K_j = \begin{cases} 1 & j = 1 \\ S_j + 1 & j > 1 \end{cases} \tag{2}$$

Recalculation of weight Q_j is as the following:

Hydrol. Earth Syst. Sci. Discuss., https://doi.org/10.5194/hess-2017-707
Manuscript under review for journal Hydrol. Earth Syst. Sci.
Discussion started: 9 February 2018

Hydrology and Earth System Sciences
Discussions

$$Q_j = \frac{X_{j-1}}{K_j} \quad (3)$$

The relative weights of the evaluation criteria are calculated by the following equation:

$$W_j = \frac{Q_j}{\sum_{j=1}^{m} Q_j} \quad (4)$$

Where W_j shows the relative weight of j-th criterion, and m stands for the total criteria number.

3.3. Groundwater spring prediction modelling

In this research, five new hybrid models namely ANFIS-DE, ANFIS-IWO, ANFIS-FA, ANFIS-PSO, ANFIS-BA were utilized for the analysis of determination of groundwater potential zonation in the study areas and for comparison between their prediction capabilities.

3.3.1. Adaptive Neuro-Fuzzy Inference System

Adaptive Neuro-Fuzzy Inference System (ANFIS) is obtained from the combination of Artificial Neural Network (ANN) and fuzzy logic (Jang, 1993). ANFIS is more efficient than the two mentioned models. Therefore, ANN has the automatic ability but is not able to explain how to get the output from decision making. Fuzzy logic, on the other hand, is the reverse of ANN by generating output from fuzzy logical decision without the ability of self-operating learning (Aghdam et al., 2017; Chen et al., 2017b; Phootrakornchai and Jiriwibhakorn, 2015). ANFIS was proposed by Jang in 1993 (Jang, 1993) to solve nonlinear and complex problems in one framework (Rezakazemi et al., 2017). This model has been used in date processing, fuzzy control and others fields (Zengqiang et al., 2008). The members of ANFIS are the function parameters from dataset for describing the system behavior (Jang, 1993). ANFIS applies to Takgi-Sugeno-Kang (TSK) fuzzy model with two rules of "If-Then" with two inputs x_1 and x_2, and one output f (Takagi and Sugeno, 1985), as follows:

$$Rule2\ 1: if\ x_1\ is\ A_1\ and\ x_2\ is\ B_1, then\ f_1 = p_1x_1 + q_1x_2 + r_1 \quad (5)$$

$$Rule\ 1: if\ x_2\ is\ A_2\ and\ x_2\ is\ B_2, then\ f_2 = p_2x_2 + q_2x_2 + r_2 \quad (6)$$

Jang's ANFIS consists of feed-forward neural network with six distinct layers. The ANFIS architecture is shown in Fig. 5. There are two shapes for nodes by different concepts in Fig.4. Fixed nodes are represented by the circular nodes and square nodes are adaptive nodes.

Hydrol. Earth Syst. Sci. Discuss., https://doi.org/10.5194/hess-2017-707
Manuscript under review for journal Hydrol. Earth Syst. Sci.
Discussion started: 9 February 2018

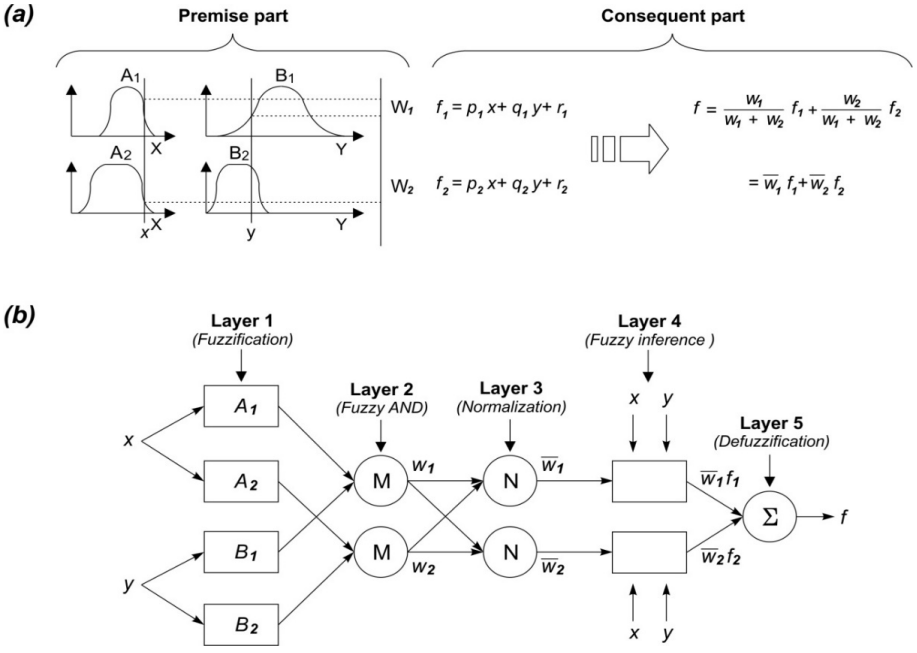

Fig.5. General ANFIS architecture of first order Takagi-Sugeno Fuzzy Model (Jang, 1993).

Layer 1 (input layer): This layer is input layer of x_1 , x_2 .

Layer 2 (fuzzification layer): Fuzzification layer converts input variables into fuzzy values and input is normalized. The parameter of i is an adaptive node with a function of $Q_{1,i}$ to compute full, none or partial membership.

$$Q_{1,i} = \mu_{A_i}(x_1) \quad for \quad i = 1,2 \tag{7}$$

$$Q_{1,i} = \mu_{B_{i-2}}(x_2) \quad for \quad i = 3,4 \tag{8}$$

Layer 3 (antecedent layer): This layer has two fixed nodes by the symbol of π to compute firing strength (w_i) or ($Q_{2,i}$) of every rule where outputs of second layer are multiplied.

$$Q_{2,i} = w_i = \mu_{A_i}(x) \times \mu_{B_i}(y) \quad for \quad i = 1,2 \tag{9}$$

Layer 4 (strength normalization layer): Fixed nodes of this layer are shown by the word of "N". These nodes apply to calculating the ratio of individual rule's firing strength to the sum of all rules' firing strengths. Output of this layer is called normalized firing strength ($Q_{3,i}$).

$$Q_{3,i} = \frac{w_i}{\sum w_i} = \frac{w_i}{w_1 + w_2} = w_i \quad for \quad i = 1,2 \tag{10}$$

Layer 5 (consequent layer): This layer is known as defuzzification layer and determines a function for each adaptive square node.

316 $$Q_{4,1} = w_i . f_i = w_i . (p_i x + q_i y + r_i) \quad for \ i = 1,2 \tag{11}$$

317 Where p_i, q_i and r_i are the consequent parameters.

318 Layer 6 (inference layer): Result of this layer is the overall output which is computed as the sum
319 of all incoming signals from the defuzzification layer by the label of "∑" in fig.5.

320 $$Q_{5,1} = \sum w_i . f_i = \frac{\sum w_i . f_i}{\sum w_i} = f_{out} \tag{12}$$

321 **3.3.2. Meta-heuristic optimization**

322 The main goal of this phase is to find the optimal antecedent and the consequent parameters of
323 the ANFIS model using IWO, DE, FA, PSO, and Bee algorithms.
324

325 **3.3.2.1. IWO algorithm**

326 Invasive weed optimization is one of the metaheuristic algorithms which mimics the colonizing
327 behavior of weeds. Its design is based on the way to find proper place for growth and reproduction
328 of weeds by Mehrabian and Locus (Mehrabian and Lucas, 2006). One characteristic of this
329 algorithm is its simplified structure; the number of input parameters is low and has strong
330 robustness. Furthermore, it is easy to understand and the same merit causes it to be used for solving
331 difficult nonlinear optimization problems (Ghasemi et al., 2014; Naidu and Ojha, 2015; Zhou et
332 al., 2015). Moreover, by comparing the results of IWO algorithm and other algorithms like SFLA
333 and PSO for solving optimization problems, IWO algorithm can compete with other ones
334 (Ghasemi et al., 2014). This algorithm consists of 4 parts as following:

335 1- Initialization

336 Random spread of some limited weeds in searching area with dimension D is considered as the
337 initial population of solutions.

338 2- Reproduction

339 Weeds are able to reproduce some seeds in accordance with their fitness during their growth. In
340 other words, the number of produced seeds from S_{min} value for weeds starts with Worst fitness
341 and then increases in linear fashion to S_{max} for them with best fitness (Fig. 6).

Hydrol. Earth Syst. Sci. Discuss., https://doi.org/10.5194/hess-2017-707
Manuscript under review for journal Hydrol. Earth Syst. Sci.
Discussion started: 9 February 2018

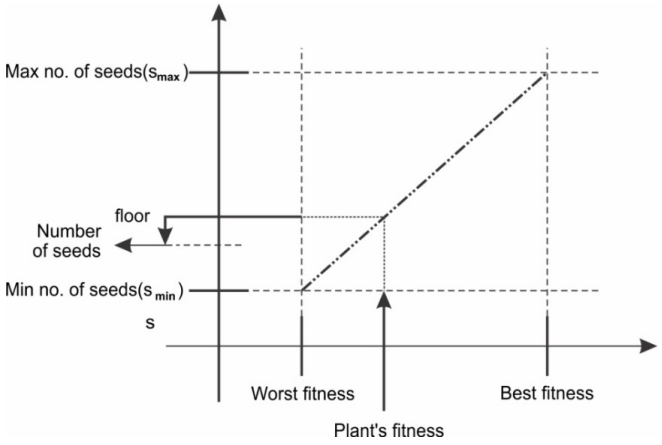

Fig.6. Seed production procedure in a colony of weeds (Mehrabian and Lucas, 2006).

3- Spatial dispersal

Produced seeds are distributed in the searching area randomly in a way that is located close to their families with normal distribution, their mean equal to zero, and different variances. Moreover, standard deviation decreases in each iteration from σ_{min} to σ_{max} and is calculated by the following non-linear equation:

$$\sigma_{iter} = \frac{(iter_{max} - iter)^n}{(iter_{max})^n}(\sigma_{min} - \sigma_{max}) + \sigma_{max} \quad (13)$$

Where $iter_{max}$ is the last iteration, σ_{iter} is the standard deviation of iteration, and n is the non-linear index considered between 2 and 3 (Saravanan et al., 2013).

4- Competitive exclusion

All weeds and their seeds combine in order to make up the population of next generation. If the population exceeds a definite maximum, those weeds with lower fitness will be removed. The reproduction mechanism and the competition provide breeding opportunity for proper weeds. If they generate fitter offspring, the offspring can survive the competition.

5- Termination Condition

Step 2 to 4 repeat in order for the iteration to reach its maximum defined value and the weeds with the best fitness will be the nearest condition to optimal solution.

3.3.2.2. DE algorithm

DE is another popular algorithm used as an evolutionary algorithm in recent years used for finding global optimal answers in a problem with continuous space (Chen et al., 2017a; Das et al., 2009). This method was first introduced by Storn and Price (Storn and Price, 1997). It is very similar to genetic algorithm that produces next optimum generation by three operators: mutation, crossover, and selection. This algorithm starts by producing random population in which each individual of

Hydrol. Earth Syst. Sci. Discuss., https://doi.org/10.5194/hess-2017-707
Manuscript under review for journal Hydrol. Earth Syst. Sci.
Discussion started: 9 February 2018

Hydrology and Earth System Sciences
Discussions

population is a symbol of solution to the problem. Vector $X_i^G = (x_{1,i}^G, x_{2,i}^G, x_{3,i}^G, \dots, x_{D,i}^G)$ shows each individual of population $i = \{0,1,2, \dots, NP\}$ is a number of each individual, in which D stands for the search dimension or in other words, is a component problem and $G = \{0,1,2, \dots, G_{max}\}$ generation time that G_{max} is the total number of generations. By assuming the maximum and minimum of every dimension of searching space, there are $X_L = \{x_{1,L}, x_{2,L}, \dots, x_{D,L}\}$ and $X_U = \{x_{1,U}, x_{2,U}, \dots, x_{D,U}\}$, respecitivly; initial population is defined as the following (Storn and Price, 1997):

$$x_{j,i}^0 = x_{j,L} + rand(0,1).(x_{j,U} - x_{j,L}) \quad (14)$$

Where $rand(0,1)$ is a uniformly distributed random number in [0, 1]

3.3.2.2.1. Mutation

The first operator in DE algorithm is mutation, which produces mutant vector $V_i^G = (V_i^G, V_2^G, \dots, V_D^G)$ by using each individual which is called target vector. Four well-known mutant operators that are used are as the following:

DE/rand/1 : $V_i^G = X_{r1}^G + F.(X_{r2}^G - X_{r3}^G)$

DE/rand/2 : $V_i^G = X_{r1}^G + F.(X_{r2}^G - X_{r3}^G) + F.(X_{r4}^G - X_{r5}^G)$

DE/best/1 : $V_i^G = X_{best}^G + F.(X_{r1}^G - X_{r2}^G)$

DE/best/2 : $V_i^G = X_{best}^G + F.(X_{r1}^G - X_{r2}^G) + F.(X_{r3}^G - X_{r4}^G)$

DE/current – to – rand/1 : $V_i^G = X_i^G + F.(X_{r1}^G - X_i^G) + F.(X_{r2}^G - X_{r3}^G)$

DE/current – to – rand/1 : $V_i^G = X_i^G + F.(X_{best}^G - X_i^G) + F.(X_{r1}^G - X_{r2}^G)$ (15)

$r1, r2, r3, r4$, are the integer numbers that have been chosen randomly from [0,NP] and the condition of $r1 \neq r2 \neq r3 \neq r4$ exists. F is the Scale factor that determines the mutation scale. It is generally selected as a random number from [0,1]. X_{best}^G is an individual that has the best fitness value in G generation.

3.3.2.2.2. Crossover

The purpose of this step is to produce trail vector (U_{ij}). Thus, this operator is defined by replacing some elements of the target vector X_i^G with mutant vector V_i^G as the following (Storn and Price, 1997):

$$U_{ij} = \begin{cases} V_{ij}^G & if\ rand\ [0,1] \leq CR\ \ or\ \ j = j_{rand} \\ X_{ij}^G & otherwise \end{cases} \quad (16)$$

Where $i \in \{1,2, \dots, NP\}$, $j \in \{1,2, \dots, D\}$, j_{rand}, is a random number from [1,D] and CR is the crossover rate which is uniformly distributed random number in [0,1].

3.3.2.2.3. Selection

Hydrol. Earth Syst. Sci. Discuss., https://doi.org/10.5194/hess-2017-707
Manuscript under review for journal Hydrol. Earth Syst. Sci.
Discussion started: 9 February 2018

Hydrology and Earth System Sciences
Discussions

Selection is characterized by comparing fitness value of U_{ij} trail vector with the target vector (X_i^G) and choosing the best ones as the next generation (Storn and Price, 1997).

$$X_i = \begin{cases} U_i^G & if\ f(U_i^G \le f(X_i) \\ X_i^G & otherwise \end{cases} \quad (17)$$

3.3.2.3. FA algorithm

Researches always try to design powerful evolutionary algorithms by utilization of swarm social behavior of animals, insects, and plants to use them for problem solving (Poursalehi et al., 2015). Firefly algorithm has been defined by Yang in Cambridge University (Yang, 2009) as an evolutionary algorithm. In recent years, many researches in different fields have taken advantage of this algorithm for optimization. The results of using FA algorithm in different problems, which require optimization, have been better than other algorithms such as SA, GA, PSO, and HAS (Alweshah and Abdullah, 2015). This algorithm is known as meta-heuristic algorithm that is originated from flashing and communication behavior of fireflies (Yang, 2009; Yang, 2010). Somewhere in the region of 2000, special firefly species exist that most of which produce short and rhythmic flashes (Zeng et al., 2015). Like in every other swarm intelligence algorithm, where their components are known as solutions for the problems, in this algorithm each firefly is a solution and its light intensity is the objective function value. In other words, a firefly with more light intensity is known as a solution. On the other hand, this firefly attracts more fireflies.

Generally, firefly algorithm follows three idealized rules as below: 1- All firefly species are unisex, with each of them attracting other fireflies without considering their gender (Amiri et al., 2013). 2- Attractiveness of a firefly is related to its light intensity. Thus, from two flashing firefly species, the one with lower light intensity moves toward the other one with higher light intensity. It should be noted that the distance between fireflies is significant because the farther they are from each other, the dimmer the light gets and the attractiveness declines exponentially (Gandomi et al., 2013). Moreover, if the light intensity of fireflies were the same; they would move randomly (Senapati and Dash, 2013). 3- Light intensity of a firefly is defined as an objective function value and must be optimized.

In order to design FA, two substantial issues are needed to be defined: light intensity variation (I) and the attractiveness' formulation (β). Fireflies' attractiveness is determined by their light intensity or brightness. In addition, brightness is associated with the objective function. The light intensity $I(r)$ varies with the distance r monotonically and exponentially as:

$$I(r) = I_0 e^{-\gamma r^2} \quad (18)$$

where I is the original light intensity, γ is the fixed light absorption coefficient and r is the distance between the two fireflies. Also, attractiveness rate is defined as below:

$$\beta = \beta_0 e^{-\gamma r^2} \quad (19)$$

where β_0 is the attractiveness when r=0. Also, the distance between two fireflies i and j with X_j and X_j is determined by the following equation:

Hydrol. Earth Syst. Sci. Discuss., https://doi.org/10.5194/hess-2017-707
Manuscript under review for journal Hydrol. Earth Syst. Sci.
Discussion started: 9 February 2018

Hydrology and Earth System Sciences
Discussions

$$r_{ij} = \|X_i - X_j\| = \sqrt{\sum_{k=1}^{d}(X_{i,k} - X_{i,k})^2} \quad (20)$$

where d is the number of the problem dimensions and $X_{i,k}$ is the $k-th$ element of the $i-th$ firefly. Also, the movement of a firefly i which is attracted to another attractive firefly j, is determined by (Yang, 2009):

$$X_i = X_i + \beta_0 e^{-\gamma r_{ij}^2}(X_j - X_i) + \alpha(rand - \frac{1}{2}) \quad (21)$$

In Eq. (21), the first and the second terms determines the attraction. However; the third term is regarded as a randomization with α, which is the step parameter, and ultimately, the rand is a random number generator which is uniformly distributed in a range from 0 to 1.

3.3.2.4. PSO algorithm

As a Meta-heuristic algorithm, PSO was first designed by Eberhart and Kennedy (Eberhart and Kennedy, 1995). Sensible characteristics of this algorithm include being powerful for optimizing the non-linear problems, its quick convergence, and relatively low calculations. These characteristics have made distinctions between this algorithm and other algorithms (Cheng et al., 2010). Thus, PSO algorithm in those problems that need optimization has a special place among researches. This algorithm has been inspired by the way the birds and fish use their collective intelligence for finding the best way to get food (Kennedy, 2011; Kennedy and Eberhart, 1995). Therefore, each bird implemented in this algorithm acts as a particle that is in fact a representative of solution to problems. These particles find the optimum answers for the problem by searching in "n" dimension space whereas "n" is the number of problem's parameters. For this purpose, particles were scattered randomly in considered space at the beginning of algorithm implementation. Then, the positioning in each iteration can improve by using equation 1 and 2 and finding better situations in that iteration and the best position of particles vector addition. Assuming that $x_i^t = (x_{i1}^t, x_{i2}^t, \dots, x_{in}^t)$ and $v_i^t = (v_{i1}^t, v_{i2}^t, \dots, v_{in}^t)$ are the position and velocity of the "$i-th$" particle in "t th" iteration, respectively. Then, position and velocity of "i th" particle in "$(i+1)$ th" iteration is calculated by summing equation 1-2 (Eberhart and Kennedy 1995).

$$v_i^{t+1} = \omega v_i^t + c_1 r_1(p_i^t - x_i^t) + c_2 r_2(g_i^t - x_i^t) \qquad with \ \ -v_{max} \le v_i^{t+1} \le v_{max}$$

$$x_i^{t+1} = x_i^t + v_i^{t+1} \quad (22)$$

where x_i^t is the last position of "i th" particle, p_i^t the best found position by "i th" particle, g_i^t the best found location by particles, r_1, r_2 the random number between 1 and 0. ω, c_1 and c_2 the inertia weight, cognitive coefficient, and social coefficient, respectively. In order to value them, many papers have been presented (Olsson, 2010) and finally the following equation has been used (Nieto et al., 2015).

$$\omega = \frac{1}{2ln2} \ \ and \ \ c_1 = c_2 = 0.5 + ln2 \quad (23)$$

It is noteworthy that the algorithm continues until the best found position by each particles unifies with the best found position of particles. In other words, all particles accumulate in one position and actually the answer to the problem is optimized.

Hydrol. Earth Syst. Sci. Discuss., https://doi.org/10.5194/hess-2017-707
Manuscript under review for journal Hydrol. Earth Syst. Sci.
Discussion started: 9 February 2018

3.3.2.5. Bee algorithm

One of the meta-heuristic algorithms designed according to bee swarm-based is Bee Algorithm. This algorithm which was first introduced by Pham (Pham et al., 2005; Pham et al., 2011) is inspired by foraging behavior of bees' colonies in search of food sources (flower patches) located near the hive. In the beginning, evenly distributed scout bees are scattered randomly in different directions to identify flower patches. After that, scout bees come back to hive and start a specific dance called waggle dance. This dance is for communicating with others in order to share the information of discovered flower patches. This information indicates direction, distance, and nectar quality of the flower patches. All the information helps the colony to have proper evaluation of all flower patches. After evaluation, scout bees come back to the location of discovered flower patches with other bees named recruit bees. Regarding the distance and the amount of nectar, different number of recruit bees are assigned to each flower patch. In other words, those flower patches with better nectar quality dedicate more recruit bees to themselves. Following that, recruit bees evaluate the quality of flower patches when performing the harvest process so that they leave the flower patches if they have low quality. Conversely, if the flower patch quality is good, it will be announced during the next waggle dance. Before implementing the BA algorithm, the following parameters need to be defined:

The number of scout bees (n), the number of patches selected out of n visited points (m), the number of best patches out of m selected patches (e), the number of bees recruited for e best patches (nep), the number of bees recruited for other (m–e) selected patches (nsp), the size of patches (ngh) and the stopping criterion.

At first, “n” number of scout bees with uniform distribution is scattered in search space randomly. Then, the algorithm starts to evaluate the fitness of those seen places by scout bees in order to define and select suitable bees as elite bees.

The sites of elite bees are selected from local search and the algorithm implements the neighborhood searches within the selected bees’ sites for the best ones where more bees exist. Only the proper bee is chosen to survive the next bee population in each site and other bees are allocated around the search space randomly to find new potential solutions. These steps continue until the algorithm convergences.

3.4. Model’s performance assessment

Forecasting error as the quantitative approaches, define as the difference between the observed and estimated values which have been used for determination of the accuracy of the performed models. In the current study the model prediction capabilities for each hybrid model in terms of spatial groundwater prediction was evaluated using Mean Squared Error (MSE) as follows (Tien Bui et al, 2016):

$$MSE = \frac{\sum_{i=1}^{n}(O_i - E_i)^2}{N} \quad (24)$$

Where O_i and E_i are observation (target) and prediction (output) values in both training and testing dataset and N is the total samples in the training or the testing dataset.

3.5. Model's performance validation and comparisons

According to Chung and Fabbari (Chung and Fabbri, 2003), validation is one of the most important steps in any spatial prediction modeling and without validation, the result of the models do not have any scientific significance. Prediction capability of these five spatial groundwater models must be evaluated using both success-rate and prediction-rate curves (Hong et al., 2015). Success-rate curves show how suitable the built model is for the groundwater potential assessment or for the evaluation of the goodness of fit (Gaprindashvili et al., 2014). Success-rate curves have been constructed using groundwater potential maps and the number of spring locations used in training dataset (Pradhan et al. 2010). Prediction rate curves which show the probabilities of the groundwater occurrences demonstrate how good the model is or evaluate the prediction power of the models. Therefore, it can be used for model prediction capabilities (Brenning, 2005). The construction procedure of prediction rate is similar to the success rate which the testing dataset (were not used in the training phase) has been used for instead of training dataset. The area under the curve (AUC) of success and prediction rate is the base for evaluation of model prediction power or assessment accuracy of the groundwater potential models quantitatively (Khosravi et al., 2016a; Khosravi et al., 2016b; Pham et al., 2017b). The AUC value varies from 0.5 to 1; the higher the AUC, the better the prediction capability of models.

3.6. Inferential statistics

3.6.1-Freidman test

As the conditioning factors have been classified into different classes, non-parametric test has been used in the current study. Non-parametric statistical procedures such as Freidman test (Friedman, 1937) have been used regardless of statistical assumptions (Derrac et al., 2011) and do not need the data to be normally distributed. The main aim of this test is to find whether there is a significant difference between the performed models or not. In other words, performing multiple comparisons to detect significant differences between the behaviors of two or more models (Beasley and Zumbo, 2003). The null hypothesis (H0) is that there are no differences among the performance of the groundwater potential models. The higher the P-value, the higher the probability that the null hypothesis is not true since if the p-value is less than the significance level (α=0.05), the null hypothesis will be rejected.

3.6.2 Wilcoxon signed-rank test

The most important drawback of Freidman test is that it only illustrates whether there is any difference between the models or not, and does not have the ability to show pairwise comparisons among performed model. Therefore, another non-parametric statistical test named Wilcoxon signed-rank test have been performed. To evaluate the significance of differences between the performed groundwater potential models, the P value and Z value have been used.

Hydrol. Earth Syst. Sci. Discuss., https://doi.org/10.5194/hess-2017-707
Manuscript under review for journal Hydrol. Earth Syst. Sci.
Discussion started: 9 February 2018

4. Result and analysis

4.1. Multi-collinearity diagnosis

Result of multi-collinearity analysis is shown in Table 1. Result has revealed that as VIF is less than 5 and the tolerance is greater than 0.1, there isn't any multi-collinearity problem among conditioning factors and all of factors are independent.

Table.1. Multi-collinearity analysis for conditioning factors

No	Groundwater conditioning factors	Collinearity Statistics	
		Tolerance	VIF
1	Slope degree	0.231	2.401
2	Slope aspect	0.206	4.270
3	Altitude	0.801	2.097
4	Curvature	0.513	1.446
5	SPI	0.410	1.689
6	TWI	0.541	2.113
7	TRI	0.328	1.939
8	Distance from fault	0.408	2.25
9	Distance from river	0.212	3.126
11	Landuse	0.296	3.891
12	Rainfall	0.298	1.686
13	Soil order	0.205	4.039
10	Geology (Unit)	0.215	4.150

4.2. Spatial relationship between springs and the conditioning factors by SWARA method

The spatial correlation between springs and the conditioning factor has been shown in Table 2. For the slope, the class of 0-5.5 degree shows the highest probability (0.45) on spring groundwater occurrences and there is a contrary correlation between slope degree and SWARA values. As the slope degree increases, the probability of spring occurrence has reduced. In the case of slope aspect, the east aspect (0.44) has the most impact on spring occurrences followed by north (0.22), west (0.177), south (0.15) and flat (0.12) in the Koohdasht- Nourabad plain. According to calculated results, in terms of altitude, the springs are the most abundant in the altitude of 1703-2068 m (0.6) and the least abundant in the altitude of 1070-1385 m (0.04). The SWARA model is high in flat areas (0.4), followed by concave (0.38) and convex (0.2). For SPI, the highest SWARA value is found for the classes of 583969-1330153 (0.46), followed by the classes of 227099-583969(0.0.23) and 48664-227099 (0.19). In the case of the TWI, the SWARA values decrease when the TWI reduces, while the highest TWI belongs to the classes of 6.6-7.9 (0.47), and the lowest is for 2.1-4.6 (0.02). There is an adverse relationship between TRI and SWARA value, and

as the TRI increases, the SWARA value reduces. The highest and the lowest values of SWARA also belongs to classes 0-8.7 (0.54) and 46.6-185 (0.001), respectively. For distance from the fault, distance less than 2000 m has the highest impact on spring occurrences and with increase in the distance (greater than 2000 m), the probability of spring occurrences has reduced. The highest SWRA value belongs to distance from the fault of 500-1000 m (0.29) and the lowest value is for greater than 2000 m (0.1). For the distance to river, it can be seen that the class of 0-200 m has the highest correlation with the spring occurrence (0.46) and there is a contrary relationship between spring occurrence and SWARA values; as the more the distance from the river, the lower the spring occurrence probability. In the case of land use, the highest SWARA values are shown for garden areas (0.219), followed by mixture of garden and agriculture (0.17), agricultural areas (0.12), whereas the lowest SWARA is for bare soil and rock (0.00063). The rainfall between 500 and 600 mm has the highest SWARA value with 0.61 and the lowest SWARA belongs to 300-400 mm (0.02). The Inceptisols have the highest SWARA values (0.5) followed by rock outcrop/Entisols (0.39), rock outcrop/Inceptisols (0.056), Inceptisoils/Vertisoils (0.028), and Badlands (0.014). The highest probability respectively belongs to the highly porous and very good water reservoir karstic oligomiocene and cretaceous pure carbonate formation (OMq and K1bl), the young and poorly consolidated highly porous detrital rock units (PeEf and Plq) and the unconsolidated quaternary alluvium (PlQc).

Table.2. Spatial correlation between conditioning factors and the spring locations by SWARA methods

Factors	Classes	Comparative importance of average value Kj	Coefficient Kj=Sj +1	wj=(X(j-1))/kj	weight wj/ sigma wj
Slope (degree)	0 - 5.55		1.000	1.000	0.454
	5.55 - 12.11	0.300	1.300	0.769	0.349
	12.11 - 19.43	1.500	2.500	0.308	0.140
	19.43 - 28.77	2.000	3.000	0.103	0.047
	28.77 - 64.37	3.500	4.500	0.023	0.010
Slope aspect	East		1.000	1.000	0.448
	North	1.000	2.000	0.500	0.224
	West	0.300	1.300	0.385	0.172
	South	0.100	1.100	0.350	0.156
	Flat	0.8	1.05	0.31	0.121
Altitude (m)	1703 - 2068		1.000	1.000	0.608
	1385 - 1703	2.200	3.200	0.313	0.190
	2068 - 3175	0.800	1.800	0.174	0.106
	531 - 1070	1.000	2.000	0.087	0.053
	1070 - 1385	0.200	1.200	0.072	0.044

Hydrol. Earth Syst. Sci. Discuss., https://doi.org/10.5194/hess-2017-707
Manuscript under review for journal Hydrol. Earth Syst. Sci.
Discussion started: 9 February 2018

	Flat		1.000	1.000	0.408
Curvature	concave	0.050	1.050	0.952	0.388
	convex	0.900	1.900	0.501	0.204
	583969.72 - 1330153.27		1.000	1.000	0.466
	227099.33 - 583969.72	1.000	2.000	0.500	0.233
SPI	48664.14 - 227099.33	0.200	1.200	0.417	0.194
	0 - 48664.14	1.000	2.000	0.208	0.097
	1330153.27 - 4136452.25	10.000	11.000	0.019	0.009
	6.64 - 7.92		1.000	1.000	0.471
	5.60 - 6.64	0.700	1.700	0.588	0.277
TWI	7.92 - 11.97	1.300	2.300	0.256	0.120
	4.63 - 5.60	0.100	1.100	0.233	0.110
	2.12 - 4.63	4.000	5.000	0.047	0.022
	0 - 5.59		1.000	1.000	0.544
	5.59 - 12.66	0.800	1.800	0.556	0.302
TRI	12.66 - 20.62	1.500	2.500	0.222	0.121
	20.62 - 30.93	3.000	4.000	0.056	0.030
	30.93 - 75.13	10.000	11.000	0.005	0.003
	0 - 200		1.000	1.000	0.242
	200 - 500	0.050	1.050	0.952	0.231
Distance from fault (m)	500 - 1000	0.100	1.100	0.866	0.210
	1000 - 2000	0.050	1.050	0.825	0.200
	> 2000	0.700	1.700	0.485	0.118
	0 - 200		1.000	1.000	0.464
	200 - 500	1.900	2.900	0.345	0.160
Distance from river (m)	500 - 1000	0.050	1.050	0.328	0.152
	1000 - 2000	0.300	1.300	0.253	0.117
	> 2000	0.100	1.100	0.230	0.107
	Garden		1.000	1.000	0.219
Land-use	mixture of garden and agriculture	0.282	1.282	0.780	0.171
	agriculture	0.340	1.340	0.582	0.128

Hydrol. Earth Syst. Sci. Discuss., https://doi.org/10.5194/hess-2017-707
Manuscript under review for journal Hydrol. Earth Syst. Sci.
Discussion started: 9 February 2018

	mixture of poor rangeland and follow	0.419	1.419	0.410	0.090
	follow	0.233	1.233	0.333	0.073
	mixture of moderate rangeland and agriculture	0.294	1.294	0.257	0.056
	mixture of very poor forest	0.124	1.124	0.229	0.050
	mixture of waterway and vegetation	0.549	1.549	0.148	0.032
	moderate forest	0.205	1.205	0.122	0.027
	mixture of agriculture with dry farming	0.064	1.064	0.115	0.025
	wood-land	0.030	1.030	0.112	0.024
	good rangeland	0.043	1.043	0.107	0.023
	rangeland	0.333	1.333	0.080	0.018
	poor rangeland	0.030	1.030	0.078	0.017
	poor forest	0.210	1.210	0.065	0.014
	moderate rangeland	0.281	1.281	0.050	0.011
	bare soil and rock	0.237	1.237	0.041	0.009
	dense rangeland	0.278	1.278	0.032	0.007
	dense-forest	10.000	11.000	0.003	0.001
	waterway	0.000	1.000	0.003	0.001
	mixture of agriculture with poor-garden	0.000	1.000	0.003	0.001
	very poor forest	0.000	1.000	0.003	0.001
	mixture of moderate forest and agriculture	0.000	1.000	0.003	0.001
	mixture of low forest and follow,	0.000	1.000	0.003	0.001
	urban and residential	0.000	1.000	0.003	0.001
Rainfall (mm)	600 - 700		1.000	1.000	0.617
	700 - 800	2.200	3.200	0.313	0.193
	800 - 900	0.600	1.600	0.195	0.121
	500 - 600	1.500	2.500	0.078	0.048
	400 - 500	1.300	2.300	0.034	0.021
Soil order	Rock Outcrops/Entisols		1.000	1.000	0.509

Hydrol. Earth Syst. Sci. Discuss., https://doi.org/10.5194/hess-2017-707
Manuscript under review for journal Hydrol. Earth Syst. Sci.
Discussion started: 9 February 2018

	Rock Outcrops/Inceptisols	0.300	1.300	0.769	0.392
	Inceptisols	5.900	6.900	0.111	0.057
	Inceptisols/Vertisols	1.000	2.000	0.056	0.028
	Bad Lands	1.000	2.000	0.028	0.014
	OMq		1.000	1.000	0.133
	PeEf	0.309	1.309	0.764	0.101
	PlQc	0.253	1.253	0.610	0.081
	K1bl	0.113	1.113	0.548	0.073
	Plc	0.014	1.014	0.541	0.072
	pd	0.059	1.059	0.511	0.068
	TRKubl	0.223	1.223	0.417	0.055
	TRJvm	0.027	1.027	0.406	0.054
	MPlfgp	0.048	1.048	0.388	0.051
	OMql	0.015	1.015	0.382	0.051
	Plbk	0.081	1.081	0.353	0.047
	E2c	0.291	1.291	0.274	0.036
	TRKurl	0.059	1.059	0.258	0.034
Lithology (unit)	Qft2	0.335	1.335	0.194	0.026
	MuPlaj	0.100	1.100	0.176	0.023
	KEpd-gu	0.080	1.080	0.163	0.022
	Kgu	0.566	1.566	0.104	0.014
	Qft1	0.064	1.064	0.098	0.013
	Ekn	0.109	1.109	0.088	0.012
	KPeam	0.027	1.027	0.086	0.011
	PeEtz	0.328	1.328	0.065	0.009
	Kbgp	0.445	1.445	0.045	0.006
	EMas-sb	0.310	1.310	0.034	0.005
	Mgs	0.626	1.626	0.021	0.003
	TRJlr	10.000	11.000	0.002	0.000
	Klsol	0.000	1.000	0.002	0.000
	JKbl	0.000	1.000	0.002	0.000

Hydrol. Earth Syst. Sci. Discuss., https://doi.org/10.5194/hess-2017-707
Manuscript under review for journal Hydrol. Earth Syst. Sci.
Discussion started: 9 February 2018

Kur	0.000	1.000	0.002	0.000
OMas	0.000	1.000	0.002	0.000
Mmn	0.000	1.000	0.002	0.000

4.3. Application of ANFIS ensemble models and model's assessment

In the current study, hybrids of ANFIS model and five meta-heuristic algorithms were designed, constructed and improved in MATLAB 8.0 software. These models are trained according to the data of other intelligent models and the amount of training and optimization is tested by using other data. All thirteen spring occurrence conditioning factors and the training dataset were applied in building the model. Methods of these models are like this: gained weights by SWARA method for each conditioning factor was fed as the input Training dataset was used for finding the correlation between SWARA values of conditioning factor and springs (were assigned to 1), and non-springs (were assigned to 0). These weights entered into a hybrid model as an output. It can find and model the relationships between input and output data and the modeling accuracy is calculated by statistical methods. The prediction ability of the five hybrid models with training dataset as a target and estimated springs pixel as an output (in a training phase) and testing dataset (in a validation phase) was shown in Fig.7 and Fig.8.

The MSE parameter indicates how much output of each hybrid's model is close to real rate. As it can be seen in Fig. 4, MSE values of ANFIS-IWO, ANFIS-DE, ANFIS-FA, ANFIS-PSO, and ANFIS-BA have been calculated for the training step 0.066, 0.066, 0.066, 0.049, and 0.09, respectively. This shows that compared to other models, ANFIS-PSO had the best performance while ANFIS-BA had the worst one for training step. However, it should be noted that training step is not adequate for determining the best model for MSE optimization, and MSE level for testing phase needs to be reviewed. According to the results shown in Fig.7, values of MSE – 0.060, 0.060, 0.060, 0.045, and 0.09 – relate to the hybrid models; ANFIS-IWO, ANFIS-FA, ANFIS-PSO, and ANFIS-BEE have been calculated and indicate that the best performance is for ANFIS-PSO, the worst for ANFIS-BA.

Hydrol. Earth Syst. Sci. Discuss., https://doi.org/10.5194/hess-2017-707
Manuscript under review for journal Hydrol. Earth Syst. Sci.
Discussion started: 9 February 2018

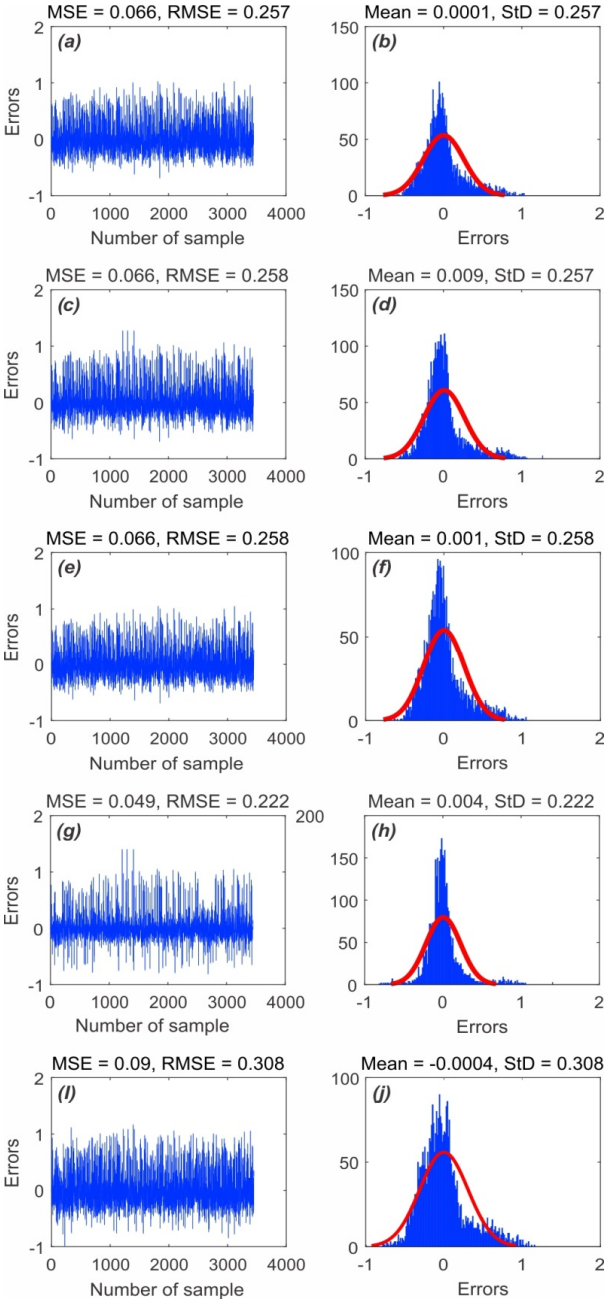

Fig. 7. MSE and RMSE values of the training data samples: a) ANFIS-IWO, c) ANFIS-DE, e) ANFIS-FA, g) ANFIS-PSO l) ANFIS-BA frequency errors of train data samples of b) ANFIS-IWO, d) ANFIS-DE, f) ANFIS-FA, h) ANFIS-PSO j) ANFIS-BA

Hydrol. Earth Syst. Sci. Discuss., https://doi.org/10.5194/hess-2017-707
Manuscript under review for journal Hydrol. Earth Syst. Sci.
Discussion started: 9 February 2018

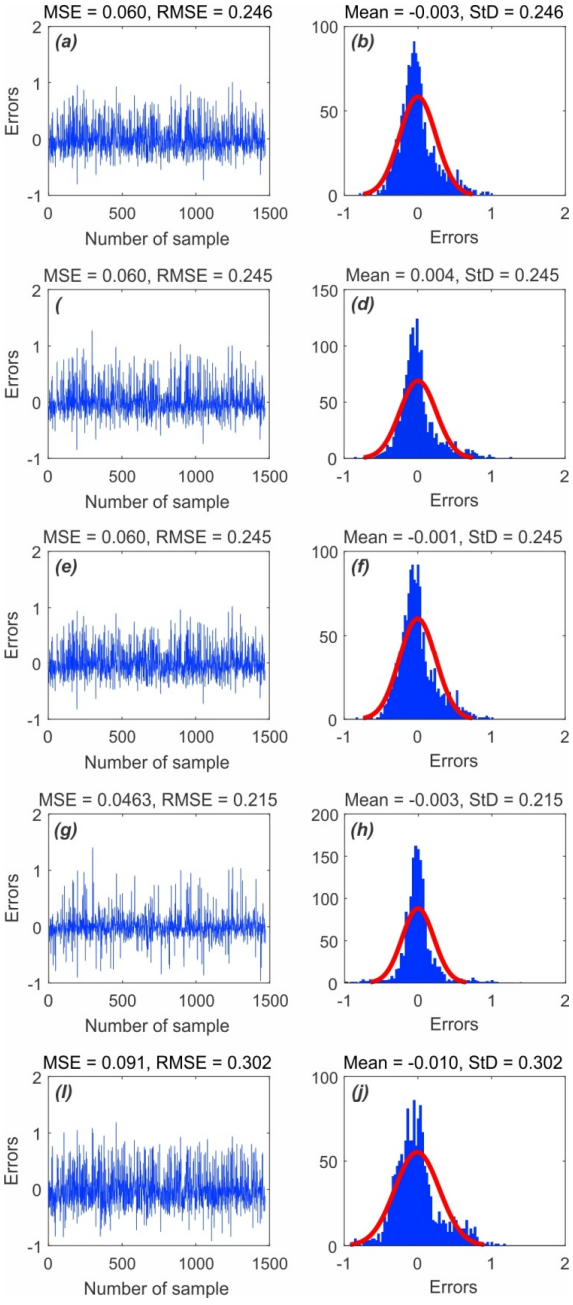

Fig.8. MSE and RMSE values of the validation data samples of a) ANFIS-IWO, c) ANFIS-DE, e) ANFIS-FA, g) ANFIS-PSO l) ANFIS-BA frequency errors of test data samples of b) ANFIS-IWO, d) ANFIS-DE, f) ANFIS-FA, h) ANFIS-PSO j) ANFIS-BA

Hydrol. Earth Syst. Sci. Discuss., https://doi.org/10.5194/hess-2017-707
Manuscript under review for journal Hydrol. Earth Syst. Sci.
Discussion started: 9 February 2018

624 However, it must be noticed that in addition to accuracy, determining the speed of used models
625 has recently found significance. To accomplish this, therefore, the processing time of 1000
626 iteration is calculated for each model where the amounts of 8036, 547, 22111, 1050, and 6993
627 seconds are related to ANFIS-IWO, ANFIS-DE, ANFIS-FA, ANFIS-PSO, and ANFIS-BA,
628 respectively (Fig. 9). As a result, it can be concluded that ANFIS-DE has had the minimum time
629 of processing speed compared to other models and ANFIS-FA has had the maximum time.

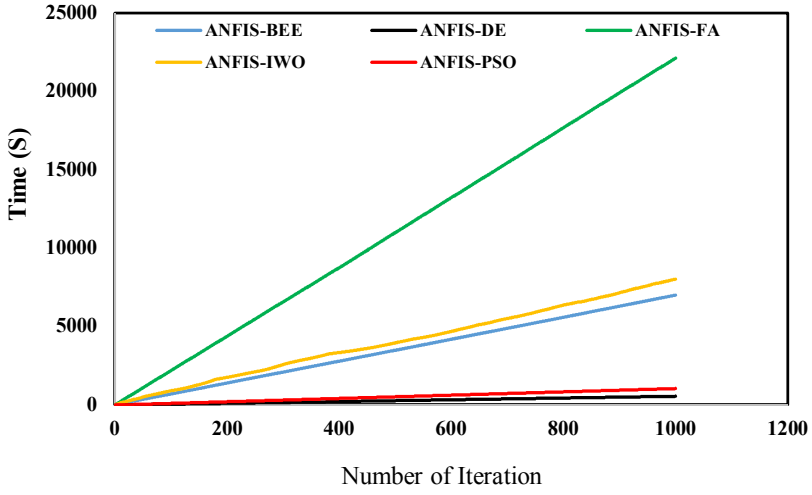

630

631 Fig. 9. Cumulative curve for speed processing of methods

632 On the other hand, it is possible to test how each model achieves convergence in learning. By
633 drawing a diagram, cost function values have been calculated in each iteration of convergence
634 graph for all five models as depicted in Fig.10. The results show that cost function values of
635 ANFIS-DE and ANFIS-BA become constant in 30 and 95 iterations. This indicates a rapid
636 convergence of every model. On the other side, ANFIS-PSO, ANFIS-IWO, and ANFIS-FA
637 achieved convergence in 650, 650, and 360 iterations, respectively that indicates the low speed of
638 these methods in reaching convergence.

Hydrol. Earth Syst. Sci. Discuss., https://doi.org/10.5194/hess-2017-707
Manuscript under review for journal Hydrol. Earth Syst. Sci.
Discussion started: 9 February 2018

Hydrology and Earth System Sciences
Discussions

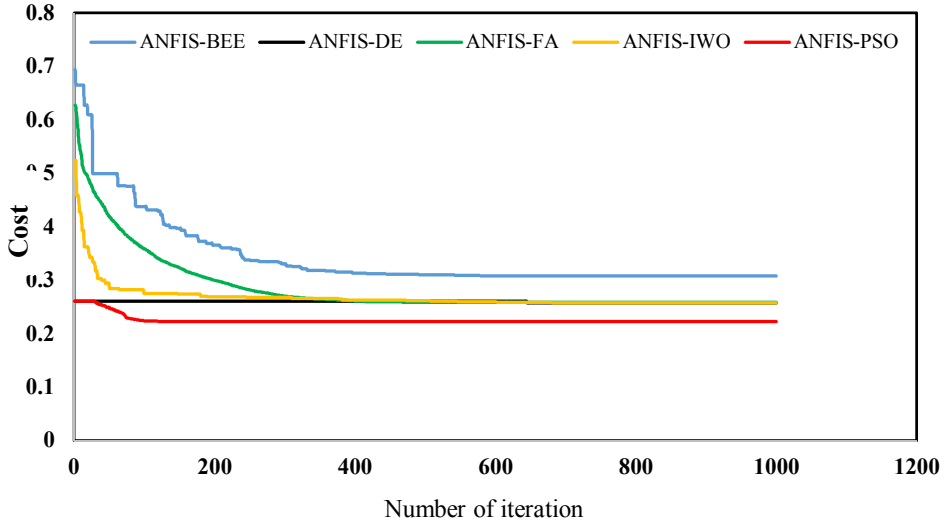

Fig.10. Convergence plot of methods

4.4. Preparation of groundwater spring potential maps using ANFIS hybrid models

In this study, SWARA values were standardized between 0-1 and were then transformed to MATLAB software. Following that, ANFIS hybrid models of ANFIS with IWO, DE, FA, PSO and BA algorithms were constructed using training dataset and standardized SWARA values. In the next step, the built models were used for estimating the groundwater spring index (GSI), which was assigned to whole the pixels of the study area and finally, the groundwater spring potential mapping was developed from groundwater spring index. At first, each pixel was assigned to a unique groundwater spring index. In second step, all indices were exported in ArcGIS10.2 software and were utilized in the construction of the groundwater spring potential mapping. Ultimately, the archived maps were divided into five potential classes, namely very low, low, moderate, high and very high based on quantile classification scheme. Therefore, based on the five hybrid model, five maps of groundwater spring potential were prepared (Fig.11 a-e). There are six methods, namely manual, equal interval, geometric interval, quantile, natural break and standard deviation for classification based on the different purposes. The selection of the best method depends on the characteristics of the data and the distribution of the groundwater spring indexes in a histogram (Ayalew and Yamagishi, 2005). If the distribution of the indexes in the histogram is normal or close to normal, two methods of Equal interval and standard deviation are used. However, if the indexes have a positive or negative skewness, the quantile or natural break classification is proper for indexes classification (Akgun, 2012). In this research, the histogram was checked and the results revealed that quantile method was better than other methods for indexes classification.

Hydrol. Earth Syst. Sci. Discuss., https://doi.org/10.5194/hess-2017-707
Manuscript under review for journal Hydrol. Earth Syst. Sci.
Discussion started: 9 February 2018

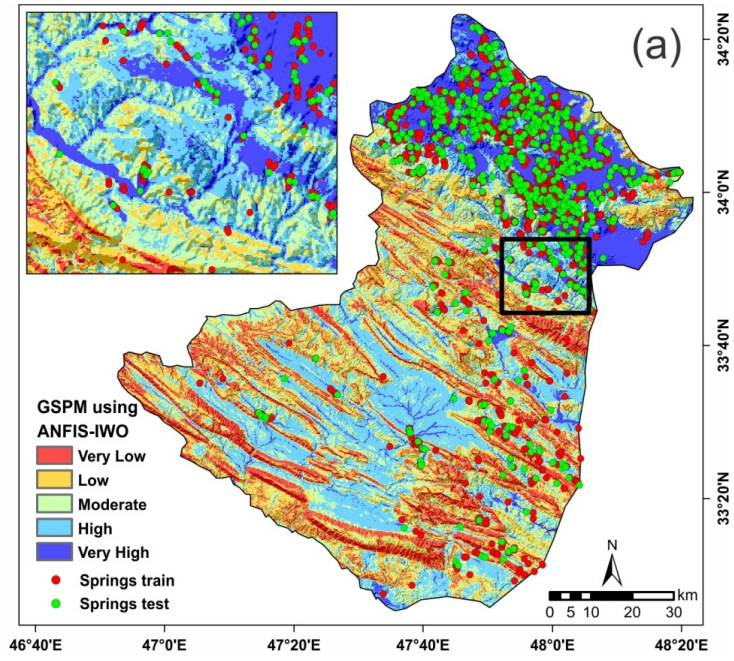

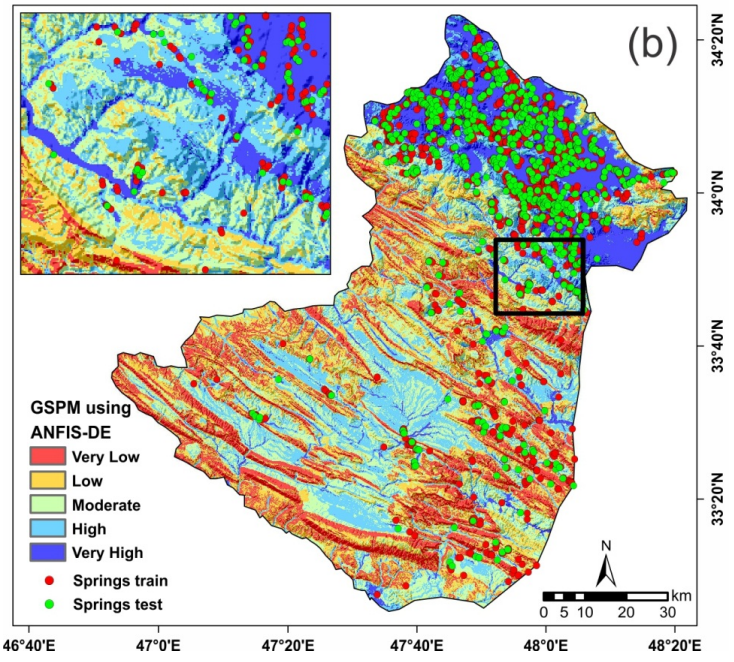

Fig.11. Groundwater spring potential mapping using ANFIS-IWO (a), ANFIS-DE (b), ANFIS-FA (c), ANFIS-PSO (d) and ANFIS-BA (e).

Hydrol. Earth Syst. Sci. Discuss., https://doi.org/10.5194/hess-2017-707
Manuscript under review for journal Hydrol. Earth Syst. Sci.
Discussion started: 9 February 2018

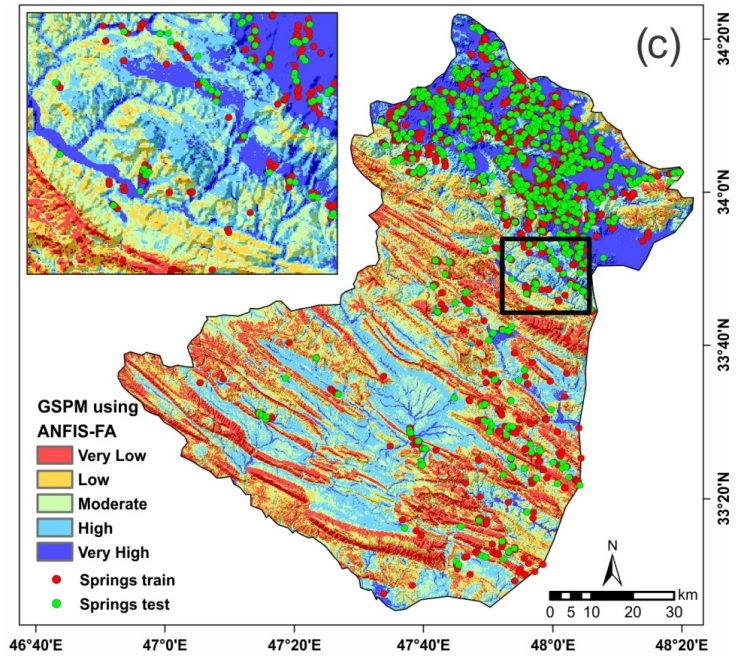

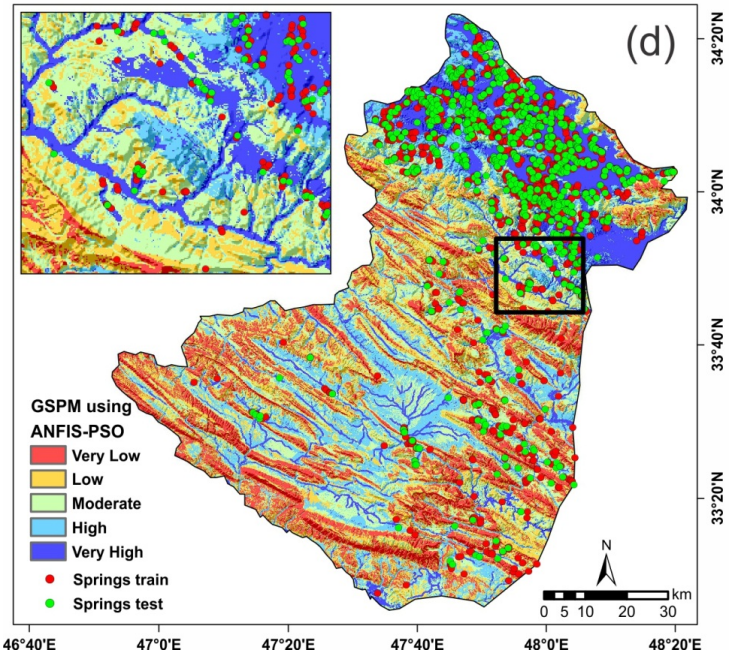

Fig.11. Continued

Hydrol. Earth Syst. Sci. Discuss., https://doi.org/10.5194/hess-2017-707
Manuscript under review for journal Hydrol. Earth Syst. Sci.
Discussion started: 9 February 2018

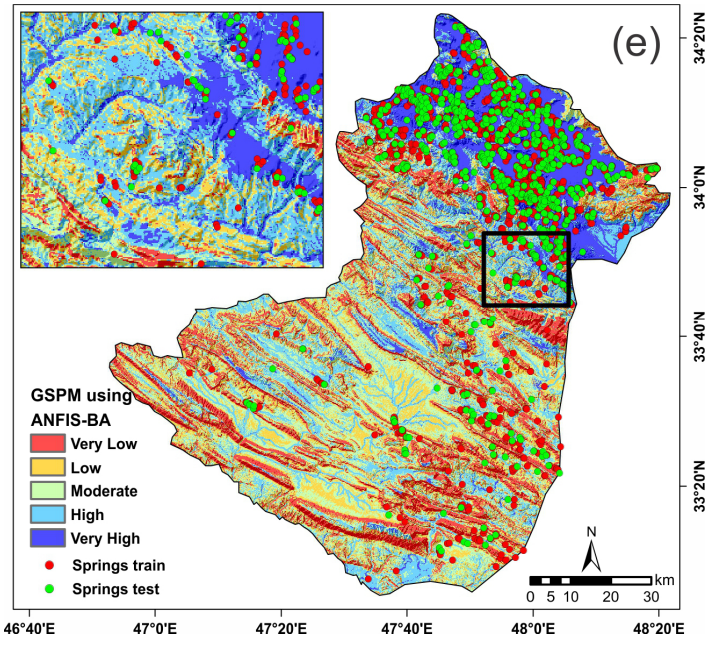

Fig.11. Continued

4.5. Validation and comparisons of the groundwater spring potential map

The prediction ability and reliability of the five achieved maps have been evaluated by both training and testing dataset. The results of the success rate revealed that the ANFIS-DE had the highest AUC value of 0.883 followed by ANFIS-IWO and ANFIS-FA (0.882), ANFIS-PSO (0.871) and ANFIS-BA (0.852) (Fig.12a). The results exhibited that all five models had a very good prediction capability but the ANFIS-DE has the highest prediction rate (0.873) followed by NFIS-IWO and ANFIS-FA (0.873), ANFIS-PSO (0.865) and ANFIS-BA (0.839), respectively (Fig.12b).

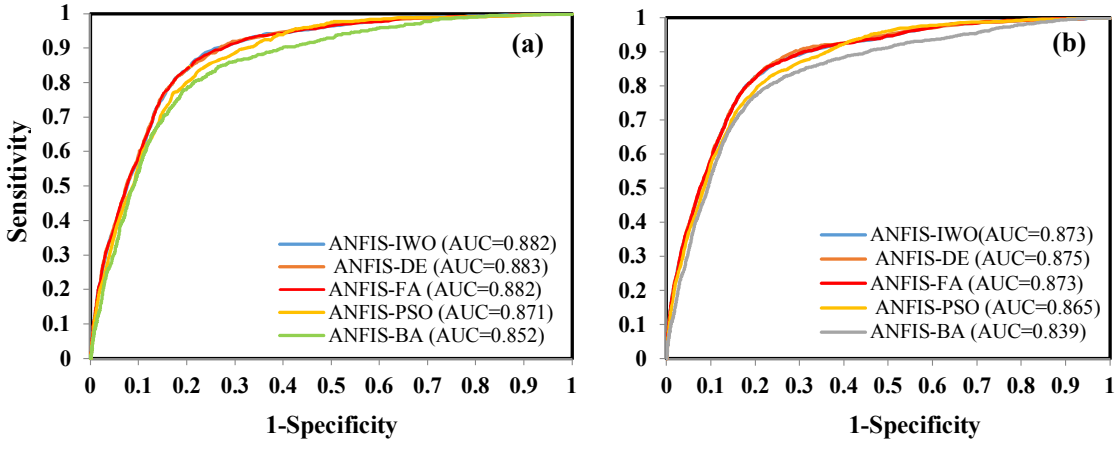

Hydrol. Earth Syst. Sci. Discuss., https://doi.org/10.5194/hess-2017-707
Manuscript under review for journal Hydrol. Earth Syst. Sci.
Discussion started: 9 February 2018

682 Fig.12. Success rate (a) and prediction rate (b) curves for the five performed models

683 **4.6. Non-parametric statistical tests**

684 The two tests of Freidman and Wilcoxon signed rank have been performed to determine whether
685 there are any statistically significant differences between the models performance or not. The result
686 of Freidman test revealed that (Table.3) as Sig and chi-square values were less than 0.05 and
687 greater than 3.84, respectively, null hypothesis has been rejected. The result also indicated that
688 there was statistically a significant difference between prediction capabilities of these five models.

689 Table.3. The result of Freidman test

NO	Performed models	Mean rank	Chi-square	Sig
1	ANFIS-DE	3.04		
2	ANFIS-IWO	3.13		
3	ANFIS-FA	2.98	64.84	0.00
4	ANFIS-PSO	2.72		
5	ANFIS-BA	3.12		

690

691 To show the pairwise differences between models performance, the Wilcoxon signed rank test was
692 carried out and result were shown in Table 4. Result of the Wilcoxon signed-rank test showed that
693 both P-values and *z* were far from the standard values of 0.05 and (from -1.96 to + 1.96),
694 respectively except for ANFIS-FA vs. ANFIS-DE and ANFIS-PSO vs. ANFIS-DE. This indicates
695 that there are statistically significant differences between models performance except for ANFIS-
696 FA vs. ANFIS-DE and ANFIS-PSO vs. ANFIS-DE.

697 Table.4. The result of Wilcoxon signed rank test

NO	Pairwise comparison	Z-Value	P-Value	Significance
1	ANFIS-DE vs. ANFIS-BA	-3.97	0.00	Yes
2	ANFIS-FA vs. ANFIS-BA	-2.37	0.017	Yes
3	ANFIS-IWO vs. ANFIS-BA	-2.35	0.018	Yes
4	ANFIS-PSO vs. ANFIS-BA	-3.04	0.002	Yes
5	ANFIS-FA vs. ANFIS-DE	-1.32	0.185	No
6	ANFIS-IWO vs. ANFIS-DE	-3.96	0.00	Yes
7	ANFIS-PSO vs. ANFIS-DE	-0.841	0.41	NO
8	ANFIS-IWO vs. ANFIS-FA	-3.19	0.001	Yes
9	ANFIS-PSO vs. ANFIS-FA	-1.90	0.057	Yes

Hydrol. Earth Syst. Sci. Discuss., https://doi.org/10.5194/hess-2017-707
Manuscript under review for journal Hydrol. Earth Syst. Sci.
Discussion started: 9 February 2018

10	ANFIS-PSO vs. ANFIS-IWO	-2.44	0.015	Yes

698

699 **4.7. Percentage area**

700 The percentage area of each class of final map resulting from five hybrid models has been
701 represented in Fig.13. According to results, as ANFIS-DE is more accurate in groundwater spring
702 prediction capabilities, the percentage areas of very low, low, moderate, high and very high
703 groundwater spring potential are about 19.06, 19.88, 21.72, 20.55 and 18.78 % of the study area,
704 respectively.

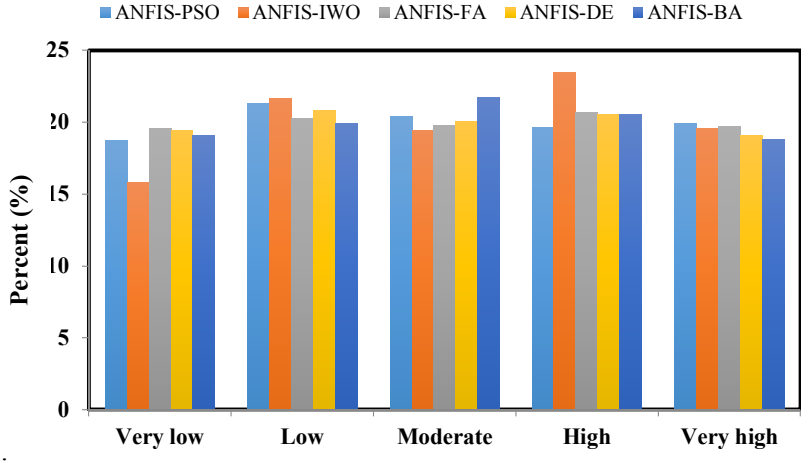

705

706 Fig.13. Percentage areas of different groundwater spring potential classes for five models

707 **5. Discussion**

708 As the most important natural resources in the world, groundwater is estimated to form around 25
709 percent of the all fresh water (Alley et al., 1999). Groundwater potential assessment has been
710 considered as one of the effective methods in the management of groundwater resources regarding
711 its better exploitation and conservation (Naghibi et al., 2017) and the prediction accuracy of the
712 achieved maps depend on the method used. Koohdasht-Nourabad plain in Lorestan province is
713 one of the most important plains in the country since majority of people in the area are farmers
714 and their water needs are met through groundwater extraction. Therefore, in the present study five
715 novel hybrid models have been applied for (1) identifying the groundwater spring potential
716 mapping with a high precision and, (2) comparing prediction capabilities of these five different
717 hybrid models in groundwater potential modeling. For achieving the aim of the current research,
718 five hybrid models of ANFIS-Invasive Weed Optimization, ANFIS-Differential Evolution,
719 ANFIS-Firefly, ANFIS-Particle Swarm Optimization and ANFIS-Bees algorithms had been used.

720 **5.1. The impact of conditioning factor's classes on GSPM**

721 The classification of conditioning factor is a necessary step in finding the correlation analysis
722 between spring and conditioning factor. It should be noted that there isn't any universal guideline

for the number and size of the classes as well as selecting the conditioning factors and they mostly depend on some factors including characteristics of the study area and previous similar studies (Xu et al., 2013). As the slope increase, the probability of the water infiltration reduces and runoff generation will increase. Thus, the more the slope, the lowest the spring occurrence probability. According to the result of the SWARA method, the springs almost occur in a middle altitude or mountain slopes (but wells are dug in a low-land area). The flat curvature retains and infiltrates rainfall. Therefore, the amount of groundwater in these areas is higher than concave or convex curvature. The east aspect has more springs than other aspects. These results are in accordance with Pourtaghi and Pourghasemi (Pourtaghi and Pourghasemi, 2014), that had explained most springs occurred in the elevation of 1600-1900 m and east slope aspect (with FR method). TWI shows the amount of wetness, and it is obvious that the more the TWI, the higher the springs probability occurrence is. Terrain Roughness Index (TRI) or topographic roughness or terrain ruggedness calculates the sum of change in elevation between a grid cell and its neighborhood, and as the lowest the roughness, the highest spring potential mapping. The SPI shows the erosive power of the water and mountainous area is higher than plain area. So, As the SPI increases, the spring potential occurrence increases. Rivers are one of the most important sources of groundwater recharge and the nearer to river, the higher probability to springs occurrences. Also, as the rainfall increases, the higher springs incident, but in the current study, some other conditioning factors affected the spring occurrences.

Most of the springs were located in the garden land-use. Therefore, it can be stated that the gardens have been established near the springs. Pliocene-Quaternary formation in a geologic time scale is newer and Quaternary formation has a high potential to groundwater springs incident due to high permeability. The fault is discontinuity in a volume of rock. Thus, the nearer to the fault, the higher the spring occurrence probability will be. Inceptisols soils are relatively new and are characterized by having only the weakest appearance of horizons, the most abundant on the Earth (https://www.britannica.com/science/Inceptisol) and mostly formed from colluvial and alluvial materials. So, due to high permeability and high rainfall infiltration, they have a high potential for springs occurrences. In the case of lithological unit, there are four suitable rock type as water reservoir based on physical phenomena such as porosity and permeability that consist of: 1. unconsolidated sands and gravels; 2. sandstones; 3. Lime-stones; and 4. basaltic lava flows. In this study area lithological units include sedimentary rocks mostly carbonate and detrital rocks with cover of alluvium and minor soil.

5.2. Advantages/disadvantages of the models and performance analysis

The highest accuracy based on the RMSE in both training and testing dataset belonged to ANFIS-PSO, but based on the AUC for success and prediction rate, the ANFIS-DE had the highest prediction capability. The problem with RMSE comes from the fact that, it is based on the error assessment. But the models should be acted upon holistically based on the abilities. AAUC for Receiver operating characteristic (ROC) curves (success and prediction rate curves) is based on the true positive (TP), true negative (TN), false positive (FP) and false negative (FN), it is more accurate than RMSE for comparison (Termeh et al., 2018). The two axes of the ROC curves are (Negnevitsky, 2005):

$$X = 1 - \text{specificity} = 1 - (\text{TN}/(\text{TN} + \text{FP})) \quad (24)$$

$$Y = \text{sensitivity} = (\text{TP}/(\text{TP}/\text{FN})) \quad (25)$$

ANFIS model is one of the machine learning algorithms that is proper for natural phenomenon modeling due to its non-linear structure. The ANFIS model, which is based on Takagi–Sugeno fuzzy inference system, is a hybrid of ANNs and fuzzy logic. Therefore, it has a potential to capture the benefits of both in a single framework and can be considered as a robust model. The predictions in ANFIS model are based on learning the ‘‘if–then’’ rules between groundwater spring locations and conditioning factors.

Polykretis et al. (Polykretis et al., 2017), applied ANFIS for landslide susceptibility mapping (LSM) in Peloponnese peninsula, Grece and stated that ANFIS model was a robust model. Vahidinia et al. (Vahidnia et al., 2010), applied ANFIS model to LSM in the Mazandaran Province, Iran, and revealed that ANFIS was a flexible and non-linear model and was completely appropriate for building a framework of easy inferences. Isanta Navarro (Isanta Navarro, 2013), applied ANFIS to stability augmentation of an airplane and stated that ANFIS had some advantages including: (1) much better learning ability, (2) need for fewer adjustable parameters than those required in other neural network structure and (3) allowing a better integration with other control design methods by its networks.

Despite several advantages of ANFIS model, non-adjutancy of membership function is the biggest disadvantage of this model. Finding the optimal parameter for neural fuzzy model in a membership function is difficult; therefore, the best parameter should be finding other optimization models. This problem was addressed in this paper for being solved by five meta-heuristic algorithms, namely Invasive Weed Optimization, Differential Evolution, Firefly, Particle Swarm Optimization and Bees algorithms. The aim of any optimization is to find values of the variable to gratify the restriction by minimizing or maximizing the objective function. These optimization algorithms are completely new in environmental modeling (especially in groundwater potential mapping) and have been used for natural hazards assessment by a few researchers in landslide susceptibility assessment (Chen et al., 2017a) as well as in flood susceptibility mapping (Bui et al., 2016; Termeh et al., 2018).

In the current study, the results showed that DE algorithm optimized the parameter for neural fuzzy model better than four other algorithms. The main DE algorithm’s advantage is its simplicity as it consists of only three parameters called N (size of population), F (mutation parameter) and C (crossover parameter) for controlling the search process (Tvrdık, 2006). Advantages of DE algorithm can be explained as follows: (1) Ability to handle non-differentiable, nonlinear and multimodal cost functions, (2) Parallelizability to cope with computation intensive cost functions, (4) good convergence properties, i.e. consistent convergence to the global minimum in consecutive independent trials, and (5) random sampling and combining vectors in the present population for creating vectors for the next generation.

Finally, it should be noted that each algorithm has some advantages or disadvantages according to the optimization problems which can be summarized as:

Some of the advantages of IWO in comparison to other evolutionary algorithms include the way of reproduction, spatial dispersal, and competitive exclusion (Mehrabian and Lucas, 2006) as well as the fact that seeds and their parents are ranked together and those with better fitness survive and become reproductive (Ahmed et al., 2014). This algorithm can benefit from combined advantages

of retaining the dominant poles and the error minimization (Abu-Al-Nadi et al., 2013) and there is no need for continuity or differentiability of the objective function.

Bees algorithm doesn't employ any probability approach, but utilizes fitness evaluation to drive the search (Yuce et al., 2013). This algorithm is implemented with several optimization problems or in other words, BA uses a set of parameters including the number of scout bees in the selected patches, the number of best patches in the selected patches, the number of elite patches in the selected best patches, the number of recruited bees in the elite patches, the number of recruited bees in the non-elite best patches, the size of neighborhood for each patch, the number of iterations and the difference between the value of first and last iterations that makes it powerful. BA also has both local and global search capability and the local search step of the algorithm covers the best locations. BA is really easy to use and available for hybridization combination with other algorithms (Yuce et al., 2013). Another advantage is hiring smart bees since bees (artificial insects) can memorize the location of the best food source and its quality which has been found before. If the new solution has a lower fitness than the best-saved solution in the SB memory, it is replaced with new candidate solution (Gorji-Bandpy and Mozaffari, 2012).

Firefly Algorithm's (FA) advantages are summarized as: (1) handling highly non-linear, multi-modal optimization problems efficiently, (2) not utilizing velocities (3) very high speed of convergence in finding the global optimized answer (4) ability to be integrated with other optimization techniques as a flexible method, and finally (5) not needing a good initial solution to beginning of its iteration process.

Advantages of Particle Swarm Optimization (PSO) algorithm can be summarized as follows: (1) Particles update themselves with the internal velocity; (2) particles have a memory important to the algorithm, (3) the 'best' particle gives out the information to others, (4) it often produces quality solutions more rapidly than alternative methods, (5) this algorithm simulates bird flocking behavior to achieve a self-evolution system, (6) it automatically searches for the optimum solution in the solution space, (7) (Wan, 2013).

As a result, there isn't any algorithm which works perfectly for all optimization problems, and each algorithm has a different performance accuracy based on different data. New algorithms, therefore, should be applied, tested and finally the most powerful algorithm should be selected; as the conclusion of the research demands.

5.3. Previous works and future work proposal

Some research has been done in groundwater well or spring potential mapping using bivariate statistical models (Al-Manmi and Rauf, 2016; Guru et al., 2017; Nampak et al., 2014) using random forest (Rahmati et al., 2016) and using boosted regression tree and classification and regression tree (Naghibi et al., 2016). The ANFIS-metaheuristic hybrid models are not used in groundwater potential mapping and are only used in flood susceptibility mapping (Bui et al., 2016; Termeh et al., 2018) and landslide susceptibility mapping (Chen et al., 2017a). Tien Bui et al. (Bui et al., 2016) ensemble the ANFIS using two optimization models, namely Genetic (GA) and PSO for the identification of flood prone areas in Vietnam. Razavi Termeh et al. (Termeh et al., 2018), used ANFIS-Ant Colony Optimization, ANFIS-GA and ANFIS-PSO in flood susceptibility mapping of Jahrom basin and stated that ANFIS-PSO had higher prediction capabilities than the two other models. Chen et al (2017) applied three hybrid models, namely ANFIS- Genetic

Algorithm (GA), ANFIS-Differential Evolution (DE) and ANFIS-Particle Swarm Optimization (PSO) for identifying the areas prone to landslides in Hanyuan County, China. The results showed that ANFIS-DE had a higher performance (AUC=0.84) followed by ANFIS-GA (AUC=0.82) and ANFIS-PSO (AUC=0.78).

Generally, the mentioned results of the present study and different researchers revealed that by applying hybrid models, better results could be achieved for any spatial prediction modeling including groundwater potential mapping. The ensembles of ANFIS by meta-heuristic algorithms can be proposed for any spatial prediction modeling such as groundwater potential mapping, flood susceptibility mapping, landslide susceptibility assessment, gully occurrences susceptibility mapping and other endeavors at a regional scale and in other areas.

For future work, it is recommended that (1) the water quality of the Koohdasht-Nourabad plain be investigated and the water quality of areas with high potential be determined for different aspects such as drinking, agricultural and industrial activities, and (2) the groundwater vulnerability assessment should be applied by some common methods including DRASTIC model for which the zones with high potential to groundwater occurrences should be preserved against pollution.

6. Conclusion

Groundwater is the most important natural resource in the world and about 25 percent of all fresh water is estimated as groundwater. Thus, the groundwater potential mapping has been considered as one of the most effective methods for the management of groundwater resources for better exploitation. The conservation and the maps with high accuracy is necessary for decisions. As the natural phenomena are complex, the simple method and statistical models do not have an appropriate result in modeling of the natural phenomena. To solve the problem, the artificial intelligence models have been used for having a reasonable result but these model have some weaknesses, especially in modeling process. To resolve this problem, this study verifies the five new hybrid models of ANFIS with metaheuristic algorithms namely IWO, DE, FA, PSO and BA to increase the prediction capability of the spatial prediction of groundwater potential mapping (1) for solving the weakness of the artificial intelligence models and (2) using non-linear structure of these models which are better for modeling of the complex natural phenomena such as groundwater modeling. The result of this modeling has been evaluated using prediction rate ROC curves and the results showed that all models had very good reasonable results. However, the ANFIS-DE had the highest prediction power (0.875) followed by ANFIS-IWO and ANFIS-FA (0.873), ANFIS-PSO (0.865) and ANFIS-BA (0.839). Thus, the results revealed that the metaheuristic algorithms could optimize the weights parameters of the ANFIS model with high accuracy as the highest advantage of these algorithms

According to the results of the SWARA method, most springs existed in an altitude of 1703-2068 m, flat curvature, east aspect, TWI of 6.6-7.9, TRI of 0-8.7, SPI of 583969-1330153, Inceptisols soil, slope of 0-5.5 degree, 0-200 m distance from river, 500-1000 m distance from fault, rainfall between 500-600 mm, in a garden, in a Pliocene-Quaternary lithological age and OMq lithology unit.

The results of the current study is helpful for Iran Water Resources Management Company (IWRMC) for sustainable management of the groundwater resources. Overall, the maps resulting from these hybrid artificial intelligence algorithms can be applied for better management of the

groundwater resources in the study area, and can be used for other areas for groundwater potential assessment or mapping of gully, flood, landslide and other susceptibility uses in the world due to its high precision.

References

Abu-Al-Nadi DI, Alsmadi OM, Abo-Hammour ZS, Hawa MF, Rahhal JS. Invasive weed optimization for model order reduction of linear MIMO systems. Applied Mathematical Modelling 2013; 37: 4570-4577.

Adiat K, Nawawi M, Abdullah K. Assessing the accuracy of GIS-based elementary multi criteria decision analysis as a spatial prediction tool–A case of predicting potential zones of sustainable groundwater resources. Journal of Hydrology 2012; 440: 75-89.

Aghdam IN, Pradhan B, Panahi M. Landslide susceptibility assessment using a novel hybrid model of statistical bivariate methods (FR and WOE) and adaptive neuro-fuzzy inference system (ANFIS) at southern Zagros Mountains in Iran. Environmental Earth Sciences 2017; 76: 237.

Ahmed A, Al-Amin R, Amin R. Design of static synchronous series compensator based damping controller employing invasive weed optimization algorithm. SpringerPlus 2014; 3: 394.

Akgun A. A comparison of landslide susceptibility maps produced by logistic regression, multi-criteria decision, and likelihood ratio methods: a case study at İzmir, Turkey. Landslides 2012; 9: 93-106.

Al-Manmi DAM, Rauf LF. Groundwater potential mapping using remote sensing and GIS-based, in Halabja City, Kurdistan, Iraq. Arabian Journal of Geosciences 2016; 9: 357.

Alimardani M, Hashemkhani Zolfani S, Aghdaie MH, Tamošaitienė J. A novel hybrid SWARA and VIKOR methodology for supplier selection in an agile environment. Technological and Economic Development of Economy 2013; 19: 533-548.

Alley WM, Reilly TE, Franke OL. Sustainability of ground-water resources. Vol 1186: US Department of the Interior, US Geological Survey, 1999.

Alweshah M, Abdullah S. Hybridizing firefly algorithms with a probabilistic neural network for solving classification problems. Applied Soft Computing 2015; 35: 513-524.

Amiri B, Hossain L, Crawford JW, Wigand RT. Community detection in complex networks: Multi–objective enhanced firefly algorithm. Knowledge-Based Systems 2013; 46: 1-11.

Ayalew L, Yamagishi H. The application of GIS-based logistic regression for landslide susceptibility mapping in the Kakuda-Yahiko Mountains, Central Japan. Geomorphology 2005; 65: 15-31.

Beasley TM, Zumbo BD. Comparison of aligned Friedman rank and parametric methods for testing interactions in split-plot designs. Computational statistics & data analysis 2003; 42: 569-593.

Berhanu B, Seleshi Y, Melesse AM. Surface Water and Groundwater Resources of Ethiopia: Potentials and Challenges of Water Resources Development. Nile River Basin. Springer, 2014, pp. 97-117.

Brenning A. Spatial prediction models for landslide hazards: review, comparison and evaluation. Natural Hazards and Earth System Science 2005; 5: 853-862.

Bui DT, Lofman O, Revhaug I, Dick O. Landslide susceptibility analysis in the Hoa Binh province of Vietnam using statistical index and logistic regression. Natural hazards 2011; 59: 1413.

Bui DT, Pradhan B, Nampak H, Bui Q-T, Tran Q-A, Nguyen Q-P. Hybrid artificial intelligence approach based on neural fuzzy inference model and metaheuristic optimization for flood susceptibilitgy modeling in a high-frequency tropical cyclone area using GIS. Journal of Hydrology 2016; 540: 317-330.

934 Bui DT, Pradhan B, Revhaug I, Nguyen DB, Pham HV, Bui QN. A novel hybrid evidential belief function-
935 based fuzzy logic model in spatial prediction of rainfall-induced shallow landslides in the Lang
936 Son city area (Vietnam). Geomatics, Natural Hazards and Risk 2015; 6: 243-271.
937 Chang F-J, Tsai M-J. A nonlinear spatio-temporal lumping of radar rainfall for modeling multi-step-ahead
938 inflow forecasts by data-driven techniques. Journal of Hydrology 2016; 535: 256-269.
939 Chen W, Panahi M, Pourghasemi HR. Performance evaluation of GIS-based new ensemble data mining
940 techniques of adaptive neuro-fuzzy inference system (ANFIS) with genetic algorithm (GA),
941 differential evolution (DE), and particle swarm optimization (PSO) for landslide spatial
942 modelling. CATENA 2017a; 157: 310-324.
943 Chen W, Pourghasemi HR, Panahi M, Kornejady A, Wang J, Xie X, et al. Spatial prediction of landslide
944 susceptibility using an adaptive neuro-fuzzy inference system combined with frequency ratio,
945 generalized additive model, and support vector machine techniques. Geomorphology 2017b;
946 297: 69-85.
947 Cheng Z, Zhou H, Yang H. Research on MPPT control of PV system based on PSO algorithm. Control and
948 Decision Conference (CCDC), 2010 Chinese. IEEE, 2010, pp. 887-892.
949 Chenini I, Mammou AB. Groundwater recharge study in arid region: an approach using GIS techniques
950 and numerical modeling. Computers & Geosciences 2010; 36: 801-817.
951 Chung C-JF, Fabbri AG. Validation of spatial prediction models for landslide hazard mapping. Natural
952 Hazards 2003; 30: 451-472.
953 Clapcott J, Goodwin E, Snelder T. Predictive Models of Benthic Macroinvertebrate Metrics. Prepared for
954 Ministry for the Environment. Cawthron Report, 2013.
955 Das S, Abraham A, Chakraborty UK, Konar A. Differential evolution using a neighborhood-based
956 mutation operator. IEEE Transactions on Evolutionary Computation 2009; 13: 526-553.
957 David Keith Todd, Mays LW. Groundwater Hydrology, 2rd Edition. Wiley, New York 1980.
958 Derrac J, García S, Molina D, Herrera F. A practical tutorial on the use of nonparametric statistical tests
959 as a methodology for comparing evolutionary and swarm intelligence algorithms. Swarm and
960 Evolutionary Computation 2011; 1: 3-18.
961 Eberhart R, Kennedy J. A new optimizer using particle swarm theory. Micro Machine and Human
962 Science, 1995. MHS'95., Proceedings of the Sixth International Symposium on. IEEE, 1995, pp.
963 39-43.
964 Fashae OA, Tijani MN, Talabi AO, Adedeji OI. Delineation of groundwater potential zones in the
965 crystalline basement terrain of SW-Nigeria: an integrated GIS and remote sensing approach.
966 Applied Water Science 2014; 4: 19-38.
967 Fitts CR. Groundwater science: Academic press, 2002.
968 Friedman M. The use of ranks to avoid the assumption of normality implicit in the analysis of variance.
969 Journal of the american statistical association 1937; 32: 675-701.
970 Gandomi AH, Yang X-S, Talatahari S, Alavi AH. Firefly algorithm with chaos. Communications in Nonlinear
971 Science and Numerical Simulation 2013; 18: 89-98.
972 Gaprindashvili G, Guo J, Daorueang P, Xin T, Rahimy P. A new statistic approach towards landslide
973 hazard risk assessment. International Journal of Geosciences 2014; 5: 38.
974 Ghalkhani H, Golian S, Saghafian B, Farokhnia A, Shamseldin A. Application of surrogate artificial
975 intelligent models for real-time flood routing. Water and Environment Journal 2013; 27: 535-
976 548.
977 Ghasemi M, Ghavidel S, Akbari E, Vahed AA. Solving non-linear, non-smooth and non-convex optimal
978 power flow problems using chaotic invasive weed optimization algorithms based on chaos.
979 Energy 2014; 73: 340-353.
980 Gorji-Bandpy M, Mozaffari A. Multiobjective optimization of irreversible thermal engine using mutable
981 smart bee algorithm. Applied Computational Intelligence and Soft Computing 2012; 2012: 5.

Güçlü YS, Şen Z. Hydrograph estimation with fuzzy chain model. Journal of Hydrology 2016; 538: 587-597.

Guru B, Seshan K, Bera S. Frequency ratio model for groundwater potential mapping and its sustainable management in cold desert, India. Journal of King Saud University-Science 2017; 29: 333-347.

Hong H, Panahi M, Shirzadi A, Ma T, Liu J, Zhu A-X, et al. Flood susceptibility assessment in Hengfeng area coupling adaptive neuro-fuzzy inference system with genetic algorithm and differential evolution. Science of The Total Environment 2017.

Hong H, Pradhan B, Xu C, Bui DT. Spatial prediction of landslide hazard at the Yihuang area (China) using two-class kernel logistic regression, alternating decision tree and support vector machines. Catena 2015; 133: 266-281.

Isanta Navarro R. Study of a neural network-based system for stability augmentation of an airplane. 2013.

Israil M, Al-Hadithi M, Singhal D. Application of a resistivity survey and geographical information system (GIS) analysis for hydrogeological zoning of a piedmont area, Himalayan foothill region, India. Hydrogeology journal 2006; 14: 753-759.

Jang J-S. ANFIS: adaptive-network-based fuzzy inference system. IEEE transactions on systems, man, and cybernetics 1993; 23: 665-685.

Jha MK, Chowdary V, Chowdhury A. Groundwater assessment in Salboni Block, West Bengal (India) using remote sensing, geographical information system and multi-criteria decision analysis techniques. Hydrogeology journal 2010; 18: 1713-1728.

Jha MK, Chowdhury A, Chowdary V, Peiffer S. Groundwater management and development by integrated remote sensing and geographic information systems: prospects and constraints. Water Resources Management 2007; 21: 427-467.

Kaliraj S, Chandrasekar N, Magesh N. Identification of potential groundwater recharge zones in Vaigai upper basin, Tamil Nadu, using GIS-based analytical hierarchical process (AHP) technique. Arabian Journal of Geosciences 2014; 7: 1385-1401.

Kennedy J. Particle swarm optimization. Encyclopedia of machine learning. Springer, 2011, pp. 760-766.

Kennedy J, Eberhart R. Particle swarm optimization, IEEE International of first Conference on Neural Networks. Perth, Australia, IEEE Press, 1995.

Keršuliene V, Zavadskas EK, Turskis Z. Selection of rational dispute resolution method by applying new step-wise weight assessment ratio analysis (SWARA). Journal of business economics and management 2010; 11: 243-258.

Khosravi K, Nohani E, Maroufinia E, Pourghasemi HR. A GIS-based flood susceptibility assessment and its mapping in Iran: a comparison between frequency ratio and weights-of-evidence bivariate statistical models with multi-criteria decision-making technique. Natural Hazards 2016a; 83: 947-987.

Khosravi K, Pourghasemi HR, Chapi K, Bahri M. Flash flood susceptibility analysis and its mapping using different bivariate models in Iran: a comparison between Shannon's entropy, statistical index, and weighting factor models. Environmental monitoring and assessment 2016b; 188: 656.

Lee M-J, Choi J-W, Oh H-J, Won J-S, Park I, Lee S. Ensemble-based landslide susceptibility maps in Jinbu area, Korea. Environmental Earth Sciences 2012; 67: 23-37.

Li Y-F, Xie M, Goh T-N. Adaptive ridge regression system for software cost estimating on multi-collinear datasets. Journal of Systems and Software 2010; 83: 2332-2343.

Lillesand T, Kiefer RW, Chipman J. Remote sensing and image interpretation: John Wiley & Sons, 2014.

Lohani A, Kumar R, Singh R. Hydrological time series modeling: A comparison between adaptive neuro-fuzzy, neural network and autoregressive techniques. Journal of Hydrology 2012; 442: 23-35.

Mehrabian AR, Lucas C. A novel numerical optimization algorithm inspired from weed colonization. Ecological informatics 2006; 1: 355-366.

1030 Mukerji A, Chatterjee C, Raghuwanshi NS. Flood forecasting using ANN, neuro-fuzzy, and neuro-GA
1031 models. Journal of Hydrologic Engineering 2009; 14: 647-652.
1032 Mukherjee S. Targeting saline aquifer by remote sensing and geophysical methods in a part of Hamirpur-
1033 Kanpur, India. Hydrogeol J 1996; 19: 53-64.
1034 Naghibi SA, Moghaddam DD, Kalantar B, Pradhan B, Kisi O. A comparative assessment of GIS-based data
1035 mining models and a novel ensemble model in groundwater well potential mapping. Journal of
1036 Hydrology 2017; 548: 471-483.
1037 Naghibi SA, Pourghasemi HR, Dixon B. GIS-based groundwater potential mapping using boosted
1038 regression tree, classification and regression tree, and random forest machine learning models
1039 in Iran. Environmental monitoring and assessment 2016; 188: 44.
1040 Naghibi SA, Pourghasemi HR, Pourtaghi ZS, Rezaei A. Groundwater qanat potential mapping using
1041 frequency ratio and Shannon's entropy models in the Moghan watershed, Iran. Earth Science
1042 Informatics 2015; 8: 171-186.
1043 Naidu YR, Ojha A. A hybrid version of invasive weed optimization with quadratic approximation. Soft
1044 Computing 2015; 19: 3581-3598.
1045 Nampak H, Pradhan B, Manap MA. Application of GIS based data driven evidential belief function model
1046 to predict groundwater potential zonation. Journal of Hydrology 2014; 513: 283-300.
1047 Nayak P, Sudheer K, Rangan D, Ramasastri K. Short-term flood forecasting with a Neurofuzzy model.
1048 Water Resources Research 2005; 41.
1049 Negnevitsky M. Artificial intelligence: a guide to intelligent systems: Pearson Education, 2005.
1050 Nieto PG, García–Gonzalo E, Fernández JA, Muñiz CD. Hybrid PSO–MARS–based model for forecasting a
1051 successful growth cycle of the Spirulina platensis from experimental data in open raceway
1052 ponds. Ecological engineering 2015; 81: 534-542.
1053 Nosrati K, Van Den Eeckhaut M. Assessment of groundwater quality using multivariate statistical
1054 techniques in Hashtgerd Plain, Iran. Environmental Earth Sciences 2012; 65: 331-344.
1055 O'brien RM. A caution regarding rules of thumb for variance inflation factors. Quality & Quantity 2007;
1056 41: 673-690.
1057 Oh H-J, Kim Y-S, Choi J-K, Park E, Lee S. GIS mapping of regional probabilistic groundwater potential in
1058 the area of Pohang City, Korea. Journal of Hydrology 2011; 399: 158-172.
1059 Olsson AE. Particle swarm optimization: Theory, techniques and applications: Nova Science Publishers,
1060 Inc., 2010.
1061 Ozdemir A. GIS-based groundwater spring potential mapping in the Sultan Mountains (Konya, Turkey)
1062 using frequency ratio, weights of evidence and logistic regression methods and their
1063 comparison. Journal of Hydrology 2011a; 411: 290-308.
1064 Ozdemir A. Using a binary logistic regression method and GIS for evaluating and mapping the
1065 groundwater spring potential in the Sultan Mountains (Aksehir, Turkey). Journal of Hydrology
1066 2011b; 405: 123-136.
1067 Pham BT, Bui DT, Pourghasemi HR, Indra P, Dholakia M. Landslide susceptibility assesssment in the
1068 Uttarakhand area (India) using GIS: a comparison study of prediction capability of naïve bayes,
1069 multilayer perceptron neural networks, and functional trees methods. Theoretical and Applied
1070 Climatology 2017a; 128: 255-273.
1071 Pham BT, Khosravi K, Prakash I. Application and comparison of decision tree-based machine learning
1072 methods in landside susceptibility assessment at Pauri Garhwal Area, Uttarakhand, India.
1073 Environmental Processes 2017b; 4: 711-730.
1074 Pham D, Ghanbarzadeh A, Koc E, Otri S, Rahim S, Zaidi M. The bees algorithm. Technical note.
1075 Manufacturing Engineering Centre, Cardiff University, UK 2005: 1-57.

1076 Pham D, Ghanbarzadeh A, Koc E, Otri S, Rahim S, Zaidi M. The bees algorithm-A novel tool for complex
1077 optimisation. Intelligent Production Machines and Systems-2nd I* PROMS Virtual International
1078 Conference (3-14 July 2006). sn, 2011.
1079 Phootrakornchai W, Jiriwibhakorn S. Online critical clearing time estimation using an adaptive neuro-
1080 fuzzy inference system (ANFIS). International Journal of Electrical Power & Energy Systems 2015;
1081 73: 170-181.
1082 Polykretis C, Chalkias C, Ferentinou M. Adaptive neuro-fuzzy inference system (ANFIS) modeling for
1083 landslide susceptibility assessment in a Mediterranean hilly area. Bulletin of Engineering
1084 Geology and the Environment 2017: 1-15.
1085 Pourghasemi H, Moradi H, Aghda SF. Landslide susceptibility mapping by binary logistic regression,
1086 analytical hierarchy process, and statistical index models and assessment of their performances.
1087 Natural hazards 2013a; 69: 749-779.
1088 Pourghasemi HR, Beheshtirad M. Assessment of a data-driven evidential belief function model and GIS
1089 for groundwater potential mapping in the Koohrang Watershed, Iran. Geocarto International
1090 2015; 30: 662-685.
1091 Pourghasemi HR, Pradhan B, Gokceoglu C. Application of fuzzy logic and analytical hierarchy process
1092 (AHP) to landslide susceptibility mapping at Haraz watershed, Iran. Natural hazards 2012; 63:
1093 965-996.
1094 Pourghasemi HR, Pradhan B, Gokceoglu C, Mohammadi M, Moradi HR. Application of weights-of-
1095 evidence and certainty factor models and their comparison in landslide susceptibility mapping at
1096 Haraz watershed, Iran. Arabian Journal of Geosciences 2013b; 6: 2351-2365.
1097 Poursalehi N, Zolfaghari A, Minuchehr A. A novel optimization method, Effective Discrete Firefly
1098 Algorithm, for fuel reload design of nuclear reactors. Annals of Nuclear Energy 2015; 81: 263-
1099 275.
1100 Pourtaghi ZS, Pourghasemi HR. GIS-based groundwater spring potential assessment and mapping in the
1101 Birjand Township, southern Khorasan Province, Iran. Hydrogeology Journal 2014; 22: 643-662.
1102 Pradhan B. Groundwater potential zonation for basaltic watersheds using satellite remote sensing data
1103 and GIS techniques. Open Geosciences 2009; 1: 120-129.
1104 Rahmati O, Pourghasemi HR, Melesse AM. Application of GIS-based data driven random forest and
1105 maximum entropy models for groundwater potential mapping: a case study at Mehran Region,
1106 Iran. Catena 2016; 137: 360-372.
1107 Rahmati O, Samani AN, Mahdavi M, Pourghasemi HR, Zeinivand H. Groundwater potential mapping at
1108 Kurdistan region of Iran using analytic hierarchy process and GIS. Arabian Journal of Geosciences
1109 2015; 8: 7059-7071.
1110 Rezaeianzadeh M, Tabari H, Yazdi AA, Isik S, Kalin L. Flood flow forecasting using ANN, ANFIS and
1111 regression models. Neural Computing and Applications 2014; 25: 25-37.
1112 Rezakazemi M, Dashti A, Asghari M, Shirazian S. H 2-selective mixed matrix membranes modeling using
1113 ANFIS, PSO-ANFIS, GA-ANFIS. International Journal of Hydrogen Energy 2017.
1114 Sander P, Chesley MM, Minor TB. Groundwater assessment using remote sensing and GIS in a rural
1115 groundwater project in Ghana: lessons learned. Hydrogeology Journal 1996; 4: 40-49.
1116 Saravanan B, Vasudevan E, Kothari D. A solution to unit commitment problem using invasive weed
1117 optimization algorithm. Power, Energy and Control (ICPEC), 2013 International Conference on.
1118 IEEE, 2013, pp. 386-393.
1119 Senapati MR, Dash PK. Local linear wavelet neural network based breast tumor classification using firefly
1120 algorithm. Neural Computing and Applications 2013; 22: 1591-1598.
1121 Shu C, Ouarda T. Regional flood frequency analysis at ungauged sites using the adaptive neuro-fuzzy
1122 inference system. Journal of Hydrology 2008; 349: 31-43.

Siebert S, Henrich V, Frenken K, Burke J. Update of the digital global map of irrigation areas to version 5. Rheinische Friedrich-Wilhelms-Universität, Bonn, Germany and Food and Agriculture Organization of the United Nations, Rome, Italy 2013.

Singh AK, Prakash SR. An integrated approach of remote sensing, geophysics and GIS to evaluation of groundwater potentiality of Ojhala sub-watershed, Mirjapur district, UP, India. Asian conference on GIS, GPS, aerial photography and remote sensing, Bangkok-Thailand, 2002.

Storn R, Price K. Differential evolution–a simple and efficient heuristic for global optimization over continuous spaces. Journal of global optimization 1997; 11: 341-359.

Takagi T, Sugeno M. Fuzzy identification of systems and its applications to modeling and control. IEEE transactions on systems, man, and cybernetics 1985: 116-132.

Tehrany MS, Pradhan B, Jebur MN. Spatial prediction of flood susceptible areas using rule based decision tree (DT) and a novel ensemble bivariate and multivariate statistical models in GIS. Journal of Hydrology 2013; 504: 69-79.

Tehrany MS, Pradhan B, Jebur MN. Flood susceptibility mapping using a novel ensemble weights-of-evidence and support vector machine models in GIS. Journal of hydrology 2014; 512: 332-343.

Termeh SVR, Kornejady A, Pourghasemi HR, Keesstra S. Flood susceptibility mapping using novel ensembles of adaptive neuro fuzzy inference system and metaheuristic algorithms. Science of the Total Environment 2018; 615: 438-451.

Tvrdık J. Competitive differential evolution and genetic algorithm in GA-DS toolbox. Technical Computing Prague, Praha, Humusoft 2006: 99-106.

Umar Z, Pradhan B, Ahmad A, Jebur MN, Tehrany MS. Earthquake induced landslide susceptibility mapping using an integrated ensemble frequency ratio and logistic regression models in West Sumatera Province, Indonesia. Catena 2014; 118: 124-135.

Vahidnia MH, Alesheikh AA, Alimohammadi A, Hosseinali F. A GIS-based neuro-fuzzy procedure for integrating knowledge and data in landslide susceptibility mapping. Computers & Geosciences 2010; 36: 1101-1114.

Waikar M, Nilawar AP. Identification of groundwater potential zone using remote sensing and GIS technique. Int J Innov Res Sci Eng Technol 2014; 3: 1264-1274.

Wan S. Entropy-based particle swarm optimization with clustering analysis on landslide susceptibility mapping. Environmental earth sciences 2013; 68: 1349-1366.

Xu C, Dai F, Xu X, Lee YH. GIS-based support vector machine modeling of earthquake-triggered landslide susceptibility in the Jianjiang River watershed, China. Geomorphology 2012; 145: 70-80.

Xu C, Xu X, Dai F, Wu Z, He H, Shi F, et al. Application of an incomplete landslide inventory, logistic regression model and its validation for landslide susceptibility mapping related to the May 12, 2008 Wenchuan earthquake of China. Natural hazards 2013; 68: 883-900.

Yang X-S. Firefly algorithms for multimodal optimization. International symposium on stochastic algorithms. Springer, 2009, pp. 169-178.

Yang X-S. Nature-inspired metaheuristic algorithms: Luniver press, 2010.

Yuce B, Packianather MS, Mastrocinque E, Pham DT, Lambiase A. Honey bees inspired optimization method: the bees algorithm. Insects 2013; 4: 646-662.

Zehtabian G, Khosravi H, Ghodsi M. High demand in a land of water scarcity: Iran. Water and Sustainability in Arid Regions. Springer, 2010, pp. 75-86.

Zeng Y, Zhang Z, Kusiak A. Predictive modeling and optimization of a multi-zone HVAC system with data mining and firefly algorithms. Energy 2015; 86: 393-402.

Zengqiang M, Cunzhi P, Yongqiang W. Road safety evaluation from traffic information based on ANFIS. Control Conference, 2008. CCC 2008. 27th Chinese. IEEE, 2008, pp. 554-558.

Zhou Y, Luo Q, Chen H, He A, Wu J. A discrete invasive weed optimization algorithm for solving traveling salesman problem. Neurocomputing 2015; 151: 1227-1236.